Плотная барионная материя и нейтронные детекторы

Ставинский А.В
НИЦ «Курчатовский Институт»-ИТЭФ,
ОИЯИ

Phase diagram of nuclear matter

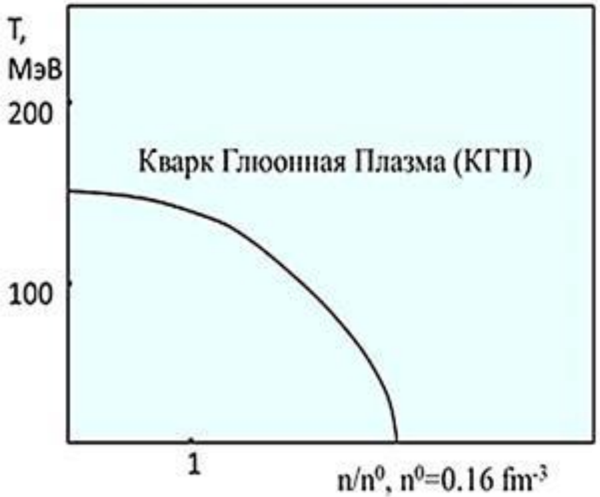

Рис.1. Представление о фазовой диаграмме ядерной материи 80-х годов прошлого века.

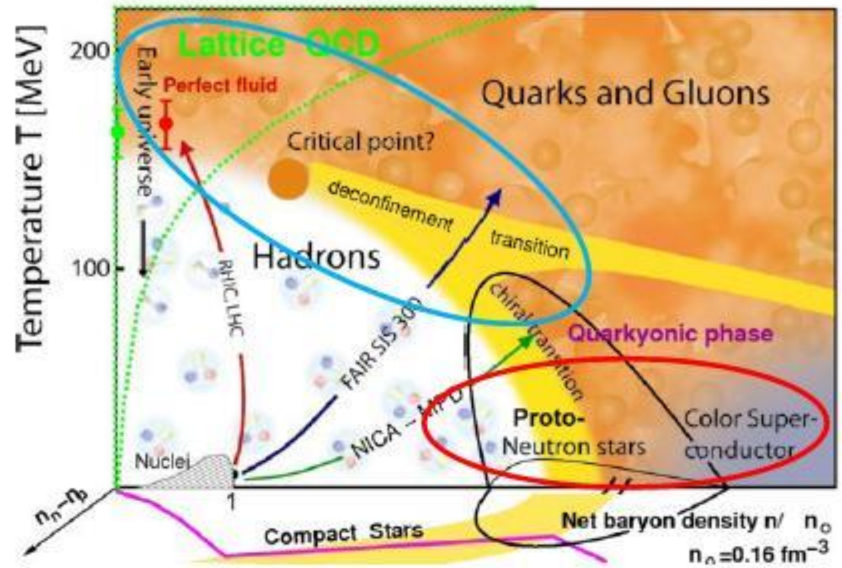

Рис.2. Современный вид фазовой диаграммы.

*current region of the experiments

**ρ/ρ_0»1, T/T_0<1(DenseColdMatter): rich structure of the QCD phase diagram - new phenomena are expected!

***Diagram study not finished-additional new phenomena can be found

See, for example L.McLerran, "Happy Island", arXiv:1105.4103 [hep-ph] and ref. therein.

An example of dense cold matter: Neutron star

Under the effect of the gravitational collapse of a core heavier than 1.4 solar masses, the matter is forced into a degenerate state: electrons are unable to remain in their orbits around the nuclei (they would have to traver faster than light in order to obey the Pauli exclusion principle) and they are forced to penetrate the
atomic nuclei. So they fuse with protons, and form neutrons. Pauli’s principle, that we've seen before, forbids two neutrons having the same state to stay in the same place . This principle creates a degeneracy pressure fighting against gravity, and so allows the remnant of the star to find an equilibrium state.The result of this process is a so called 'neutron star', whose diameter is about 10 to 20 kilometers, weighting as much as the Sun.

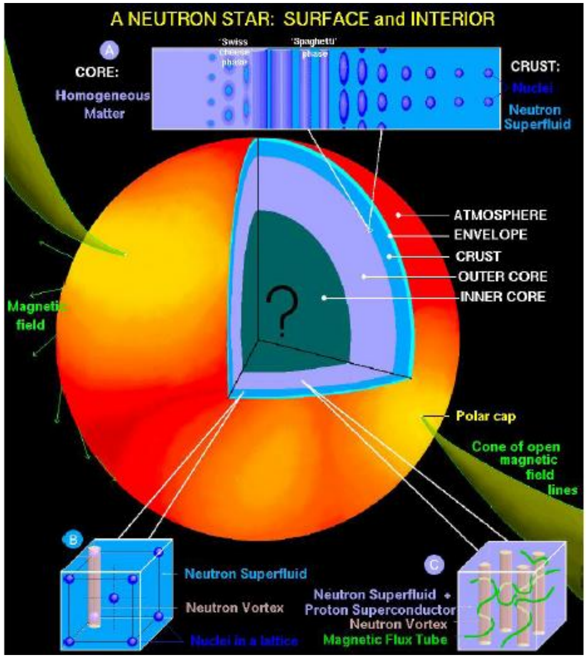

Only in the most primitive conception, a neutron star is constituted from neutrons.
At the densities that exist in the interiors of neutron stars, the neutron chemical potential, μ_n, easily exceeds the mass of the so that neutrons would be replaced with hyperons. This would happen for neutron Fermi momenta correspond to densities of just $\sim 2\rho_0$, with $\rho_0 = 0.16\ \mathrm{fm}^{-3}$ the baryon number density of infinite nuclear matter.(F.Weber et.al.,astro-ph/0604422)

*strangeness enhancement in DCM
**exotic(dibaryons, pentaquarks,…)

CC,UrQMD,10^5 ev.	2AGeV	3AGeV	4AGeV	10AGeV	30AGeV
All particles	2968383	3269875	3555732	4785049	6861519
P	980372	973357	964317	934470	899765
N	982267	974936	965797	937139	900696
Λ	1393	5493	10405	30537	57559
Σ^+	489	2347	4389	11135	17909
Σ^0	623	2918	5653	12424	19557
Σ^-	549	2277	4321	11209	18108
π^+	178772	269480	354107	714208	1286150
π^0	205822	312142	407661	796030	1418912
π^-	178205	267809	354088	713459	1286178
K^+	1607	6884	13574	45080	108427
K^0	1506	6741	13218	44376	108090
antiK^0	30	279	942	11760	51677
K^-	27	279	918	11516	51639

3AGeV: $K^+ + K^0$ (13625) ~ $\Lambda+\Sigma$(13035).

Motivation: the QGP

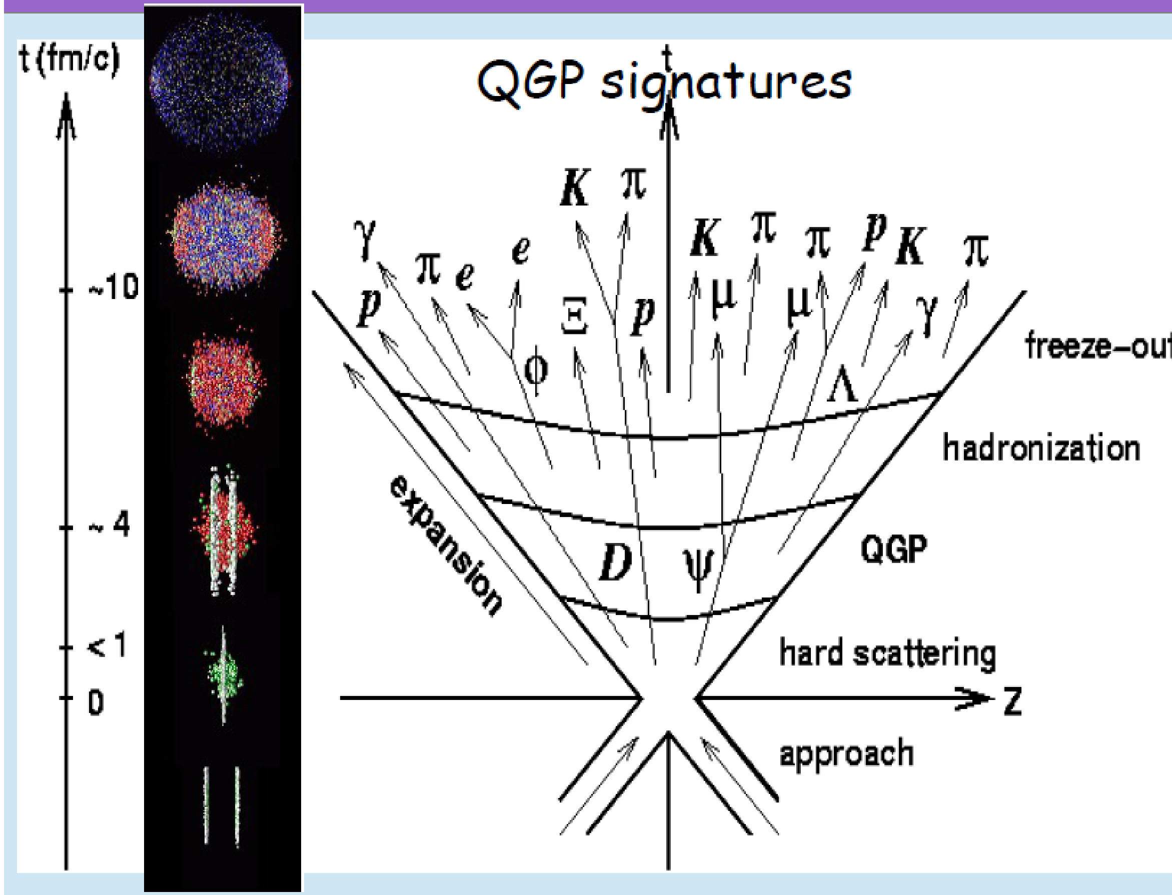

Kinetic: no elastic collisions

Chemical: no inelastic collisions

First bound states

Thermalized medium

Heavy quarks + jets + direct photons

Why no neutrons? Strange baryons:Λ,Ξ^-. Why no $\Sigma(\Sigma^-,\Sigma^0,\Sigma^+)$?

Σ^+ DECAY MODES Fraction ($\Gamma i/\Gamma$)

$p\pi^0$ (52 %)

$n\pi^+$ (48 %)

Σ^0 DECAY MODES Fraction ($\Gamma i/\Gamma$)

$\Lambda\gamma$ (100 %)

Σ^- DECAY MODES Fraction ($\Gamma i/\Gamma$)

$n\pi^-$ (100 %)

To identify Σ one needs detectors for γ and n.

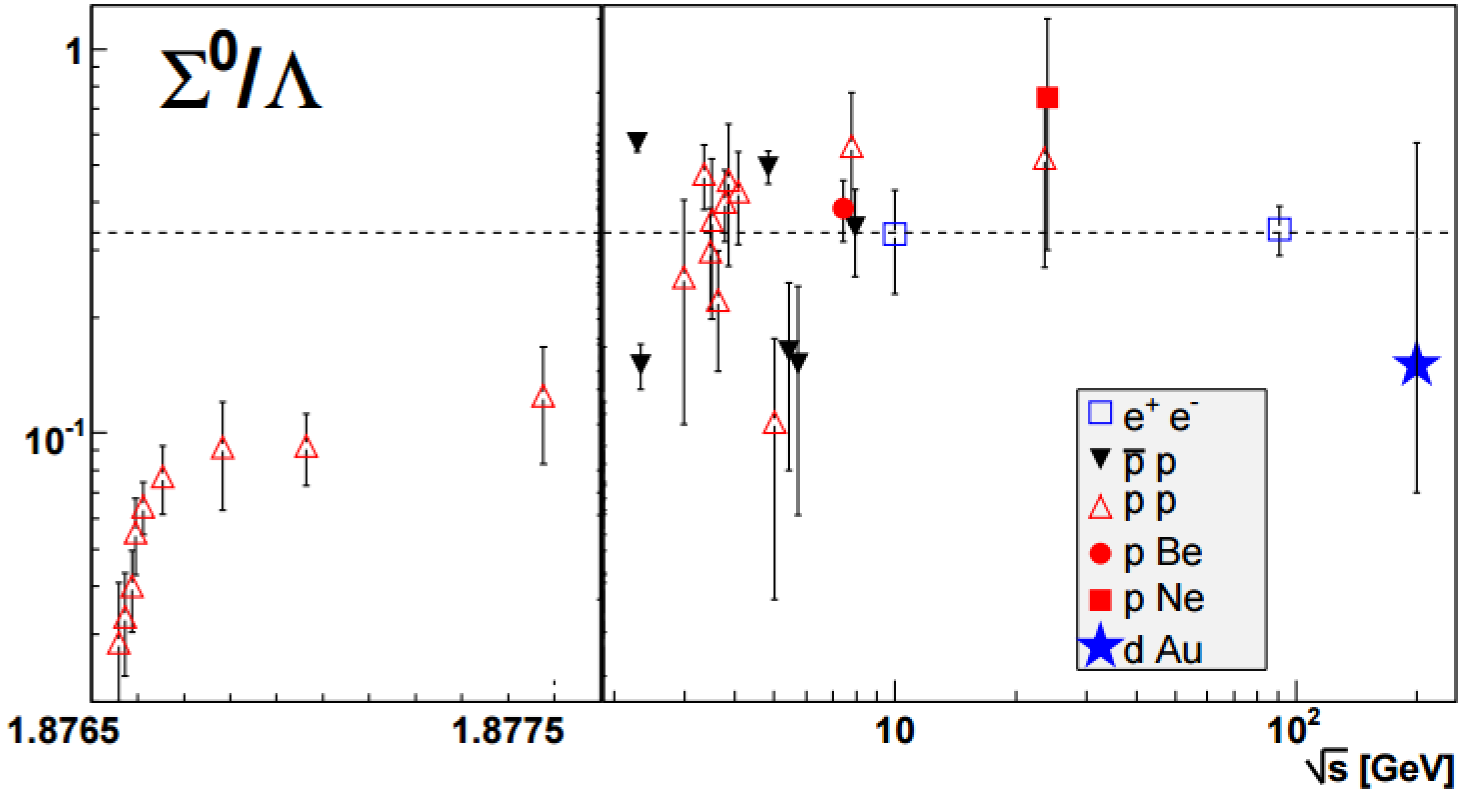

Figure 4: Σ^0/Λ results versus collision $\sqrt{s}$ ($\sqrt{s_{NN}}$ for p/d+A) [1]. Meson-nucleon reaction results are excluded for clarity, but exist only at intermediate energies and lie in the same range. The dashed line is the ratio of isospin degeneracy factors (1/3).

arXiv:nucl-ex/0512018,G.Van Buren for the STAR collaboration

FSI depends on the size of the interaction region(~$1/r^2$) , Λ/Σ ($E \rightarrow 0$) 3 for AA in contrast to Λ/Σ ($E \rightarrow 0$) 30 for pp? No data!

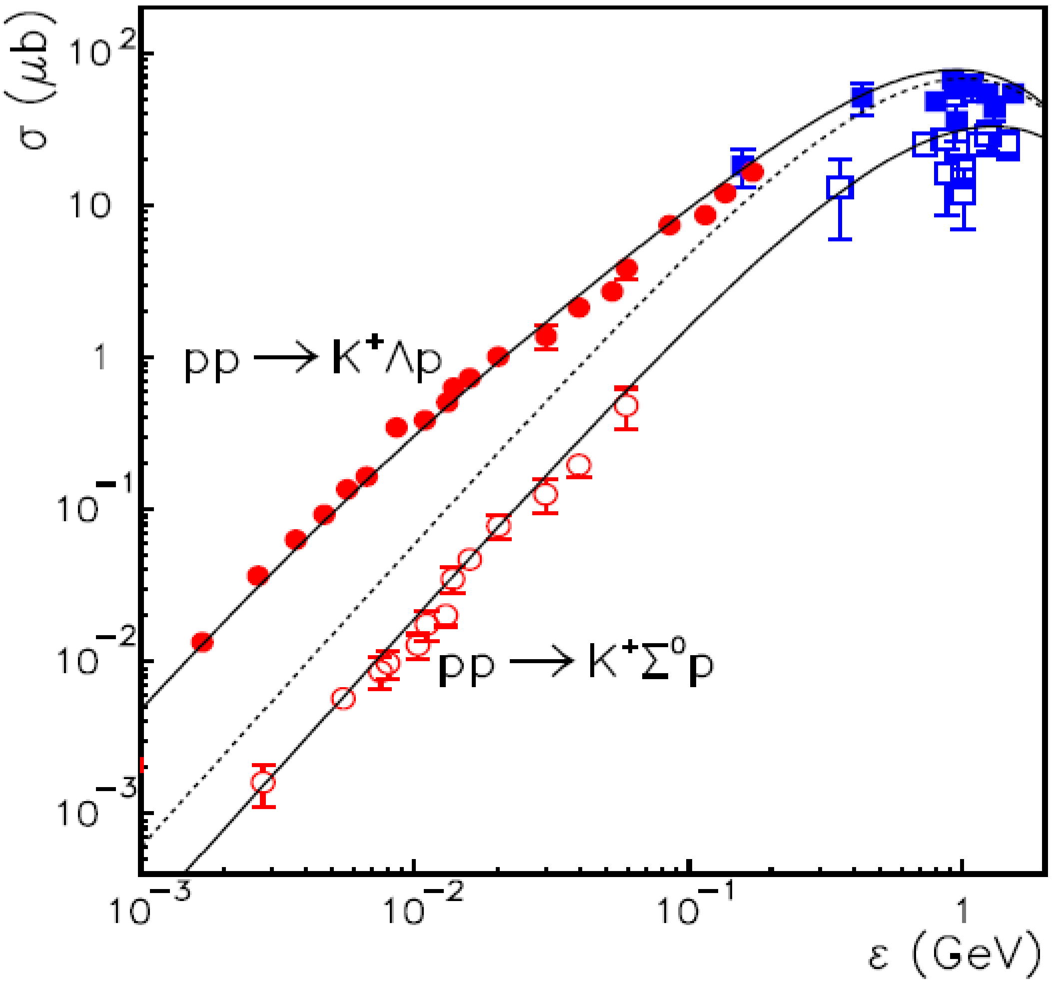

Fig. 1. Total cross sections for the $pp \to K^+ \Lambda p$ (closed symbols) and $pp \to K^+ \Sigma^0 p$ (open symbols) reactions as a function of the excess energy ϵ. Results from COSY [1,2,11,13,14] are indicated by circles, while the squares are data from Ref. [25]. The solid lines are our results for the Λ and Σ^0 reaction channels, respectively. The dashed line is obtained by switching off the Λp final-state interaction.

arXiv:hep-ph/0608098, A.Sibirtsev et al.

No FSI for Σ ?

E»1GeV(no FSI)

Model baryon=quark+diquark:
“ diquark: T=S=1 or 0.”
И.Ю.Кобзарев, Б.В.Мартемьянов, М.Г.Щепкин
УФН 162, вып.4,1992,стр.1-41
See, also, Anisovich A.V., et al., Int. J. Modern Phys. A, 25:15 (2010);
arXiv:1001.1259[hep-ph]
(**Quark**-**Diquark Systematics of Baryons)**

From: Craig Roberts <cdroberts.phy.anl@gmail.com>

…independent of detailed information about the interaction used to describe quark-quark scattering.

The result is most easily seen when looking at Eqs. (A.1) in [[arxiv.org]https://arxiv.org/pdf/1705.03988.pdf]. There you will see that the isospin=0 Lambda contains two different arrangements of diquark correlations. However, the simple [ud] configuration is forbidden in the isospin=1 Sigma^0, which only contains [us]d+[ds]u. To be explicit, here are the flavour wave function components:
Lambda ... [ud]s, [us]d-[ds]u, {us}d-{ds}u
Sigma^0 ... [us]d+[ds]u, {us}d+{ds}u

Dynamics determines the relative strength of each term within a given baryon.
As you note below, depending on the assumed reaction mechanism, this difference in diquark content could affect the Lambda/Sigma production ratio in AA collisions.

Σ+(uus)/Σ-(dds) ratio is ideal instrument for the study of electromagnetic effects

Coulomb correction in classical approximation(Gyalassy M.,Kaufmann S.K.,Nucl.Phys.1981,A362,p.503), see also discussion in L.S.Vorobiev,G.A.Lexin, A.S.(Yad.Fiz. 1996,v.59, n.4, p.694)

$V \sim Z_1 * Z_2 e^2/r$; $r \sim 2$fm, $Z_2 = \pm 1$, $0 < Z_1 < Z_{A1} + Z_{A2}$

$\delta V_{\Sigma+\Sigma-}$ (max) ~ 0.3 Mev(p+p), 2MeV(C+C), 6Mev(Ar+KCl), 11Mev(Kr+Cu), 28MeV(Au+Au)

For comparison: $M_{\Sigma+\ (1189,37)} - M_{\Sigma-(1197,45)} \sim 8$ MeV

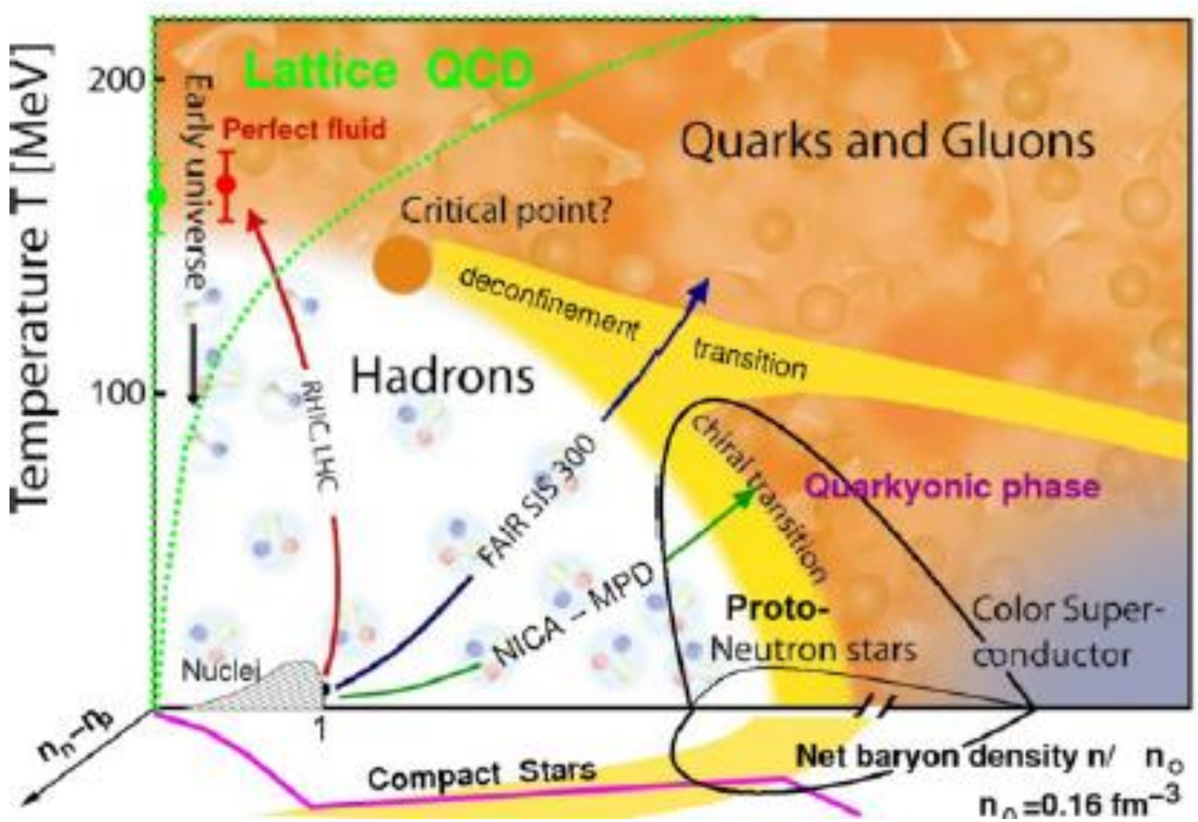

Let's consider cold and dense fermion rich system with u/d≠1.
"cold" means small internal energy per degree of freedom $E \ll m_\pi$
"dense" means $\delta p \delta x \sim \hbar$
N_n must to be ~ N_P due to Pauli blocking
Strong deviation ∑-(dds)/∑+(uus) ratio from 1 could be a solution

DCM detector(project version), AA plane

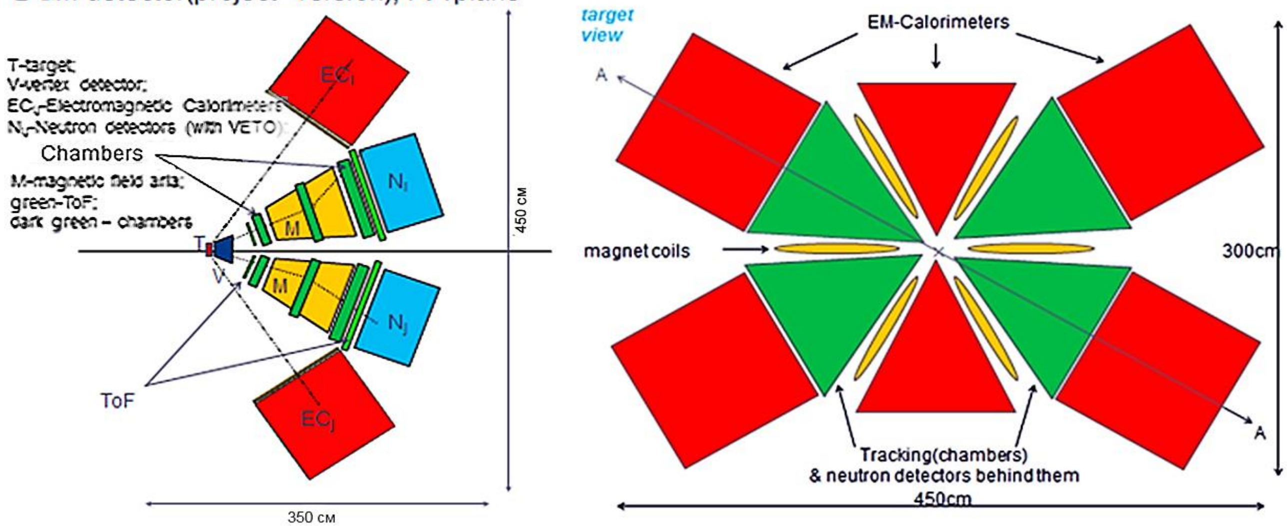

DeMoN detector

Time resolution ~ 250 psec
Efficiency ~ 30-40%

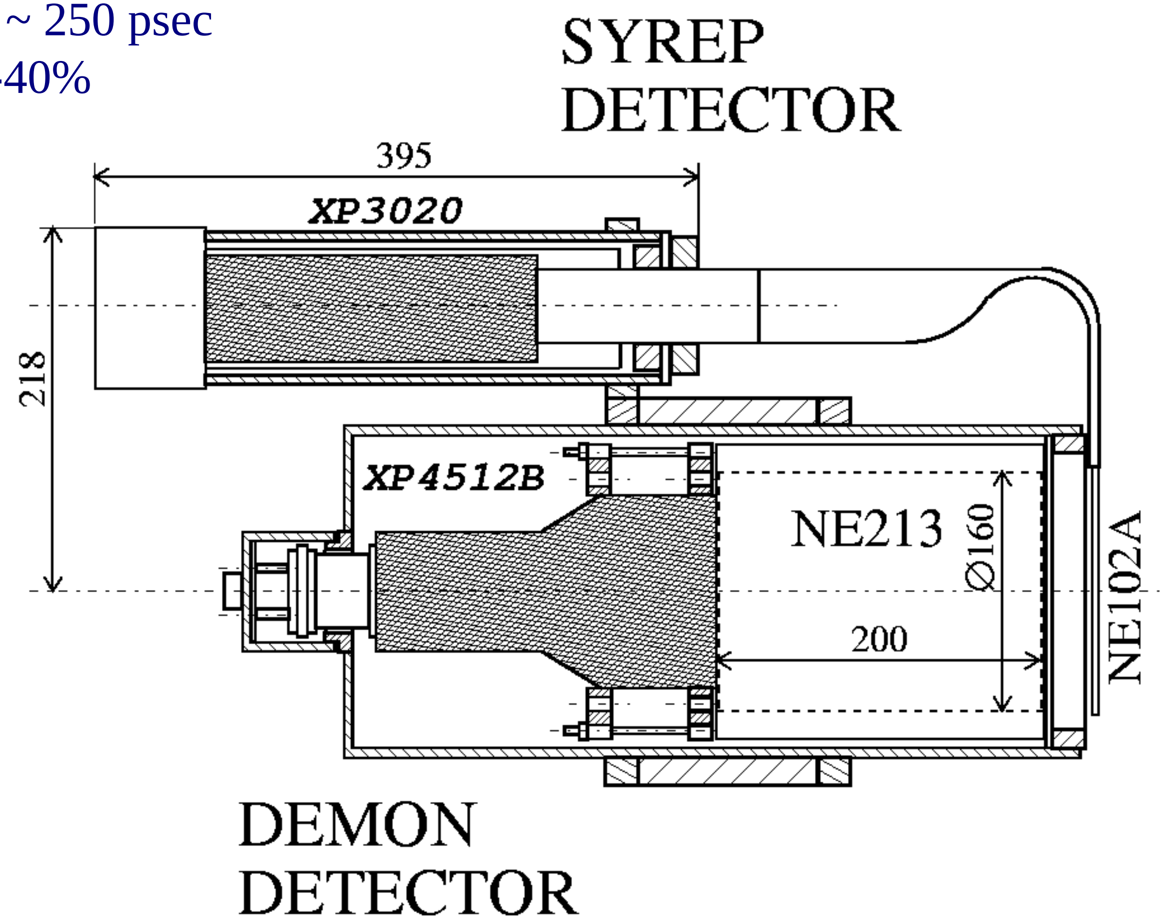

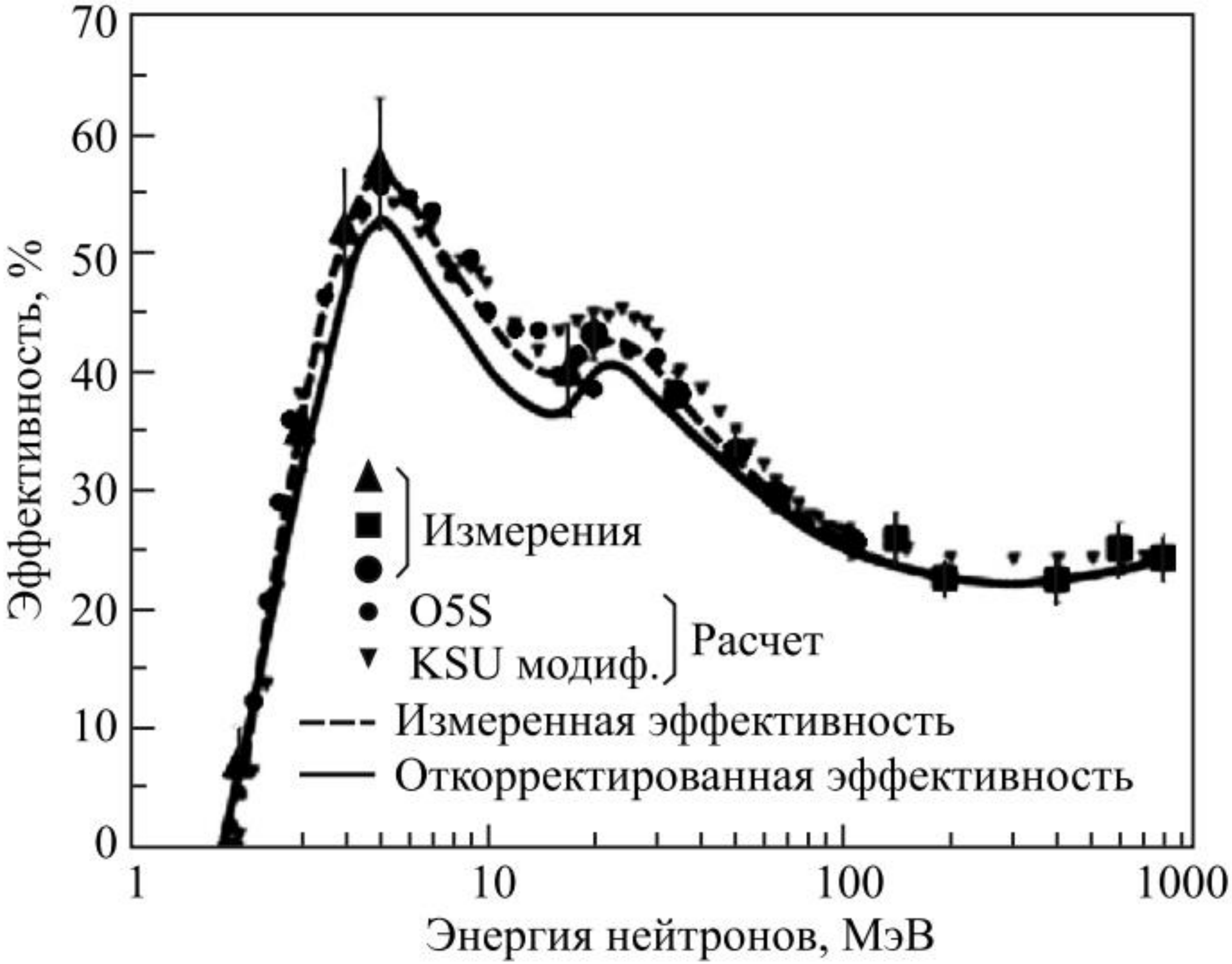

70
60
50
40
30
20
10
0
Эффективность, %
1
10
100
1000
Энергия нейтронов, МэВ
Измерения
O5S
KSU модиф.
Расчет
Измеренная эффективность
Откорректированная эффективность

E286 experiment

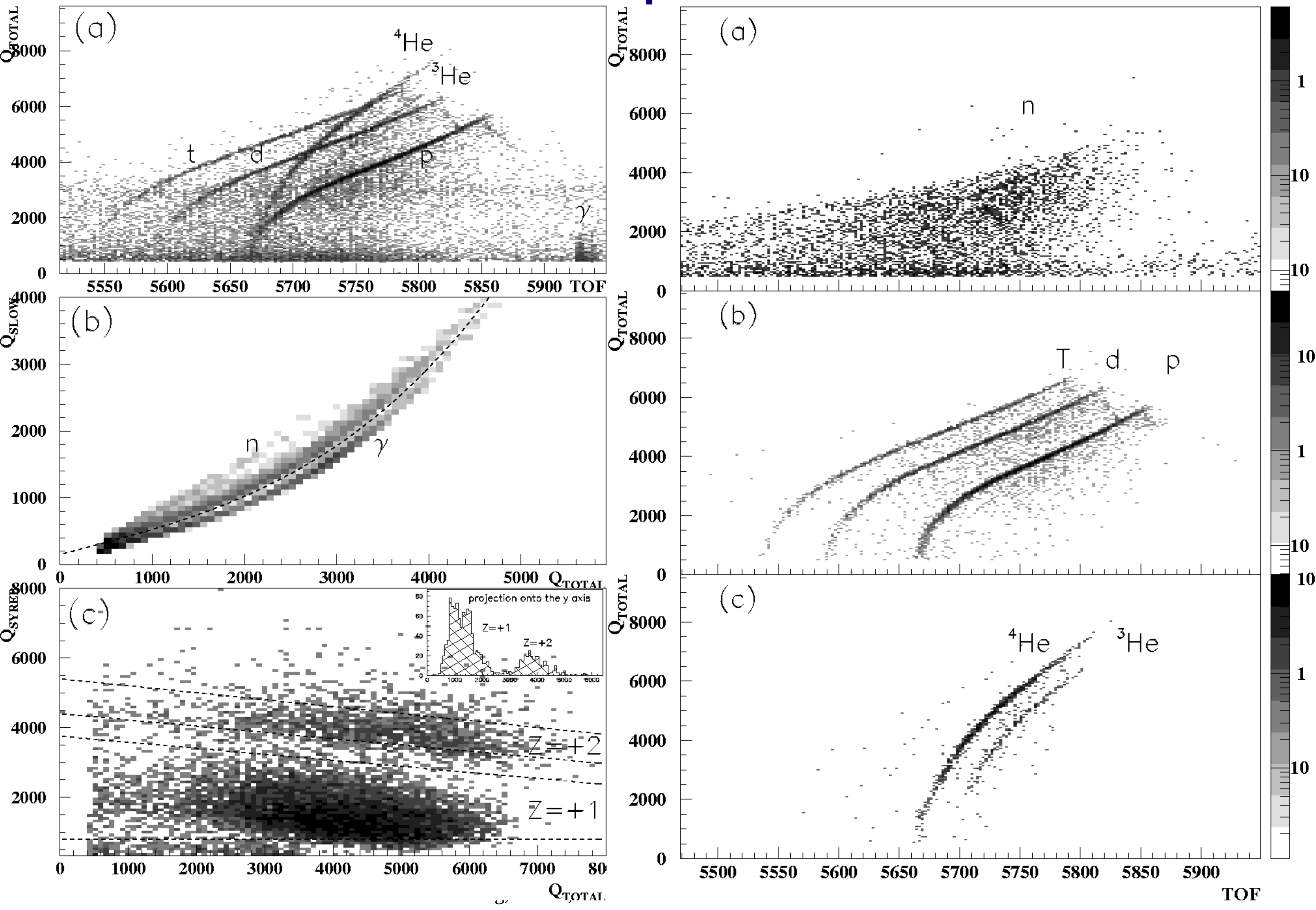

LAND

Large area detector for high-energy neutrons

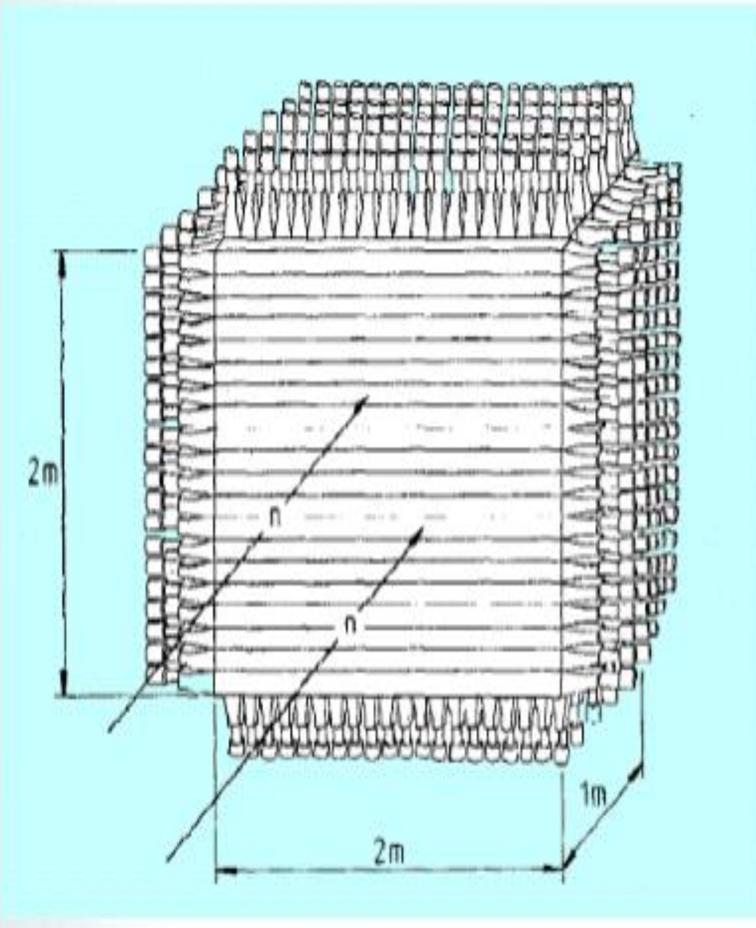

$\Delta Tn/Tn$ = 5.3% for neutrons of
Tn = 1 GeV
and angular resolution: 0.2°
for a flight path of 15 m

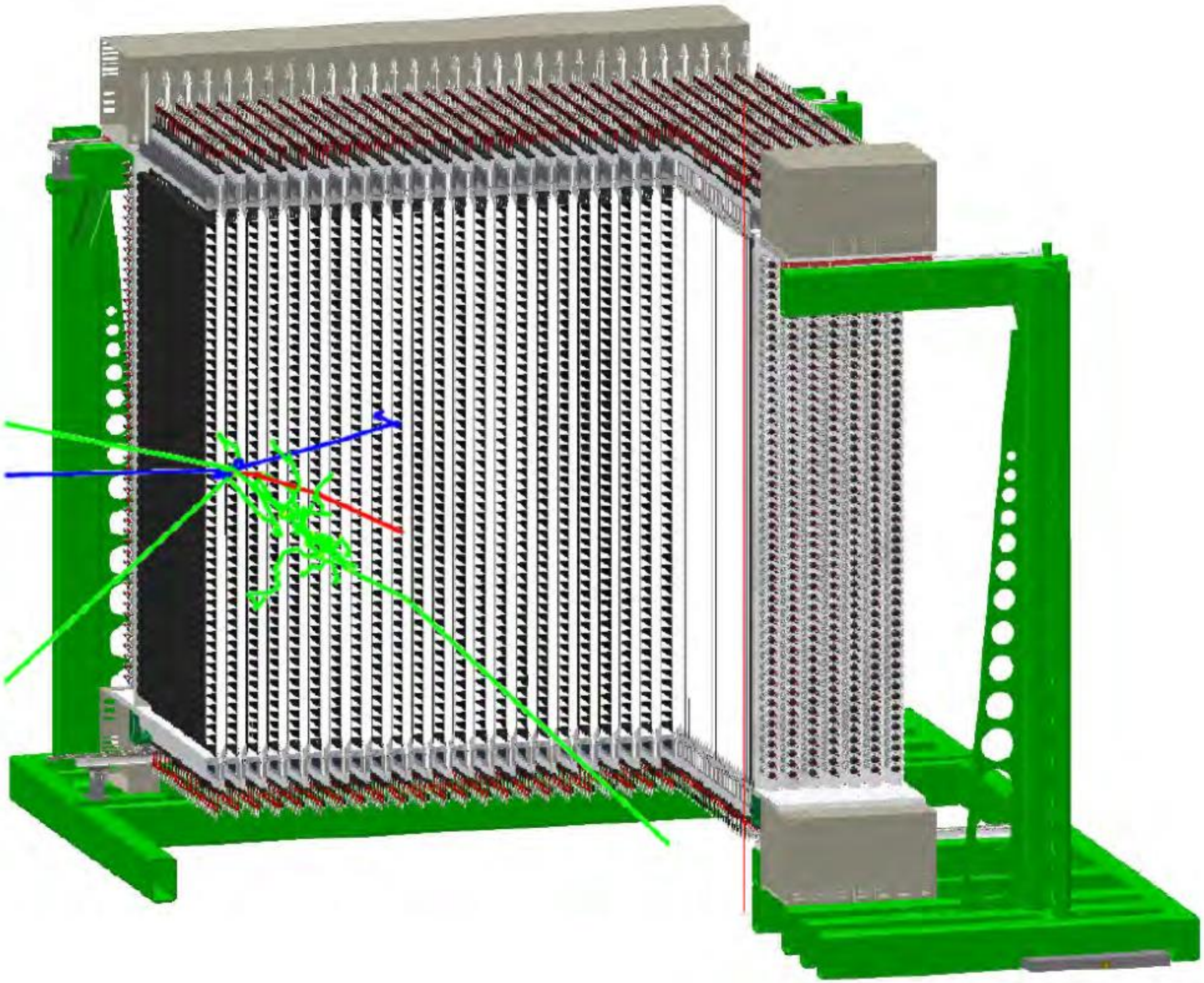

NeuLAND collaborating institutes

Croatia:RBI Zagreb ; **Germany**: GSI Darmstadt,HZDR Dresden-Rossendorf,
TU Darmstadt,TU Dresden,U Cologne,U Frankfurt
Hungary:MTA Debrecen,Eötvös Lóránd University; **Netherlands:**KVI-CART, Groningen ;
Portugal: LIP Coimbra,U Lisbon; **Romania**: ISS Bucharest; **Russia**: PNPI St. Petersburg
Sweden: Chalmers Univ. of Technology, Göteborg

Neutron ToF Spectrometer NeuLAND

General Information

NeuLAND (new Large-Area Neutron Detector) is the next-generation neutron detector designed for R^3B which meets all requirements defined by the ambitious physics program proposed for the R^3B facility. NeuLAND features a high detection efficiency, a high resolution, and a large multi-neutron-hit resolving power. This is achieved by a highly granular design of plastic scintillators, avoiding insensitive converter material. The detector will consist of 3000 individual submodules with a size of 5x5x250 cm^3, arranged in 30 double planes with 100 submodules providing an active face size of 250x250 cm^2 and a total depth of 3 m. NeuLAND can be divided into two detectors for special applications and can be placed at different distances from the target, in order to meet specific experimental demands. A momentum resolution of $\Delta p/p$ of 10^{-3} similar to that for the charged particles is desired, resulting in resolution requirements for the time of flight of $\sigma(t) < 150$ ps and a position resolution of $\sigma(x,y,z) \approx 1.5$ cm for given flight paths in the range from 10 to 35 m. For an experiment on a medium mass nucleus at about 500 MeV/nucleon, invariant-mass resolutions of about ΔE =20 keV at 200 keV above the neutron threshold (ΔE=30 keV at 1 MeV respectively) will be reached using the maximum flight path. Apart from the excellent energy resolution of NeuLAND, the enhanced multi-neutron recognition capability with an efficiency of up to ~50% for a reconstructed five-neutron event at 1 GeV (see tabels below) will constitute a major step forward.

Neutron detector (prototype 1)-ITEP

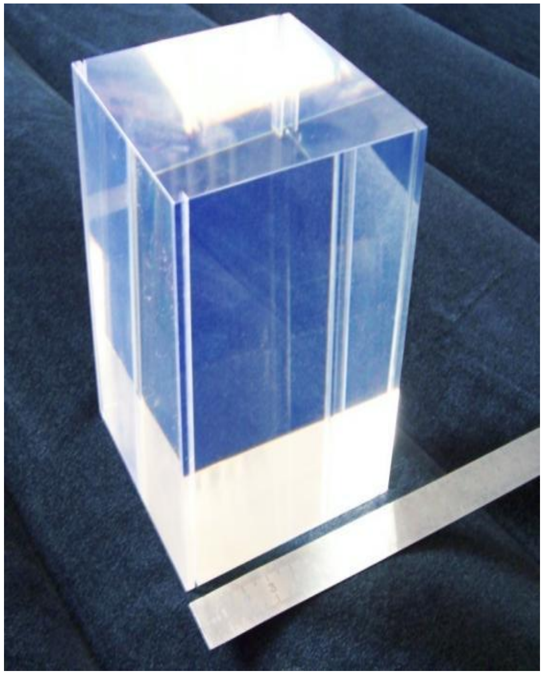

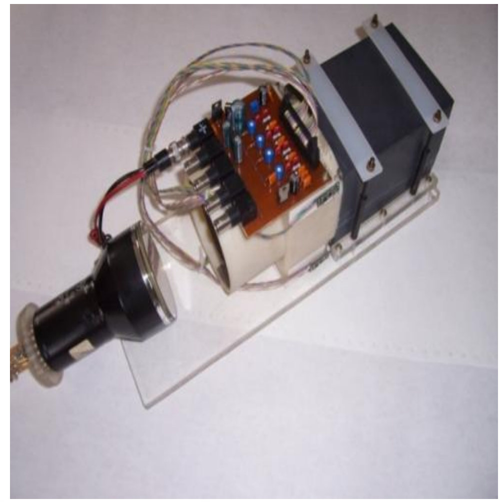

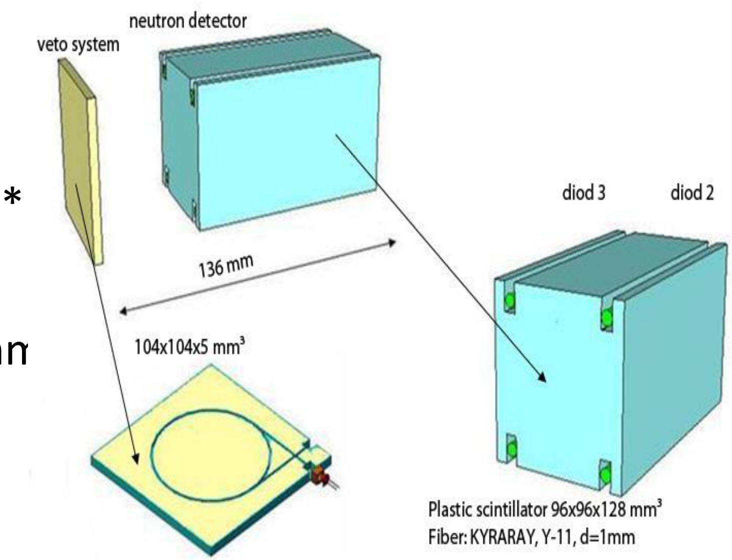

Plastic Scintillator 96 * 96 * mm^3

Fiber: KYRARAY,Y-11,d =1mm

wavelength shift

4 SiPM & Amplifier - CPTA(Golovin)

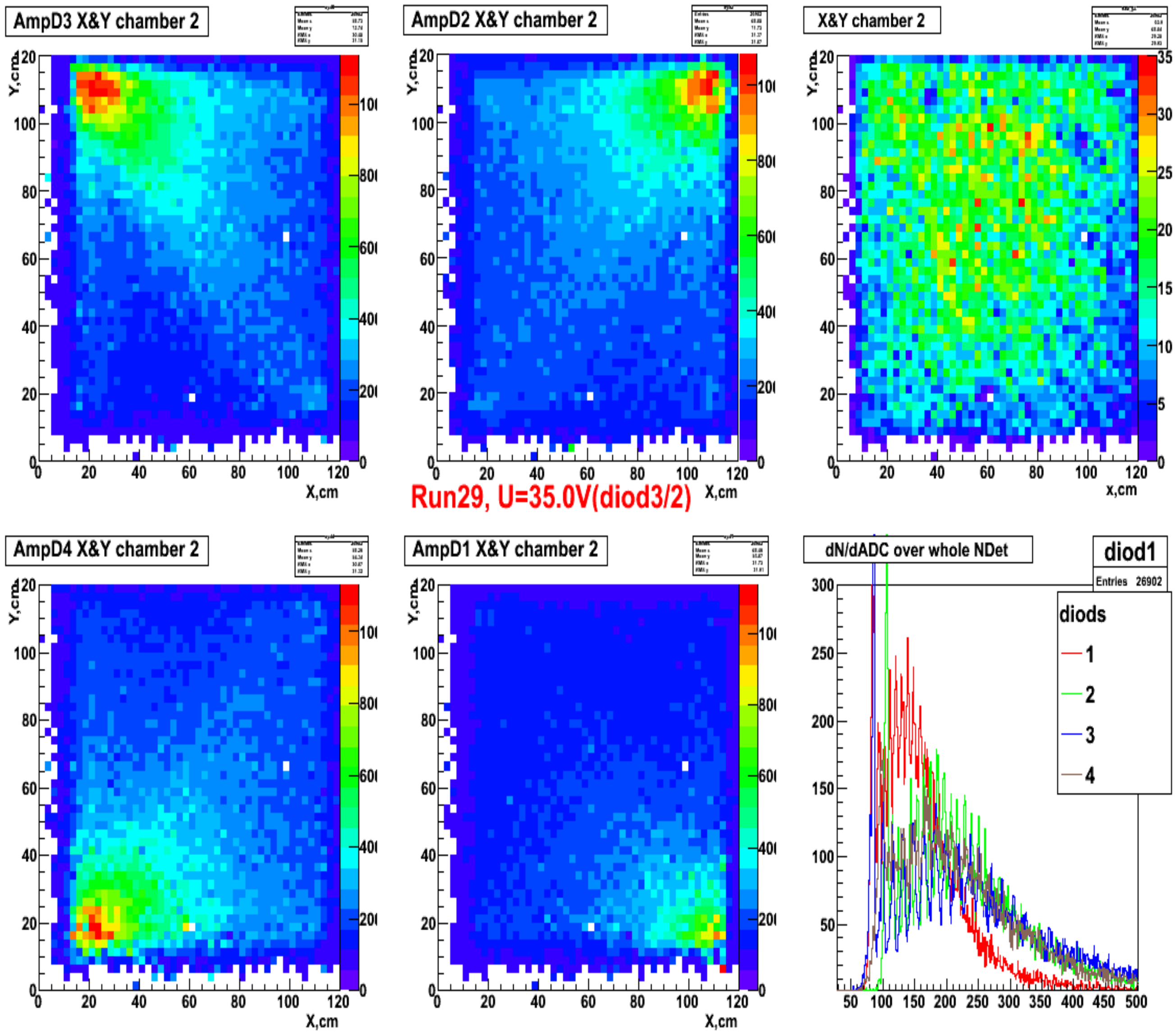
AmpD3 X&Y chamber 2
AmpD2 X&Y chamber 2
X&Y chamber 2
Run29, U=35.0V(diod3/2)
AmpD4 X&Y chamber 2
AmpD1 X&Y chamber 2
dN/dADC over whole NDet
diod1
Entries 26902
diods
1
2
3
4
Y,cm
X,cm
x,cm

Позиционно-чувствительный нейтронный детектор

Назначение: идентификация нейтронов и заряженных ядерных фрагментов в диапазоне кинетических энергий 5-200 МэВ.

(ИТЭФ - ОИЯИ)

Модуль в процессе сборки

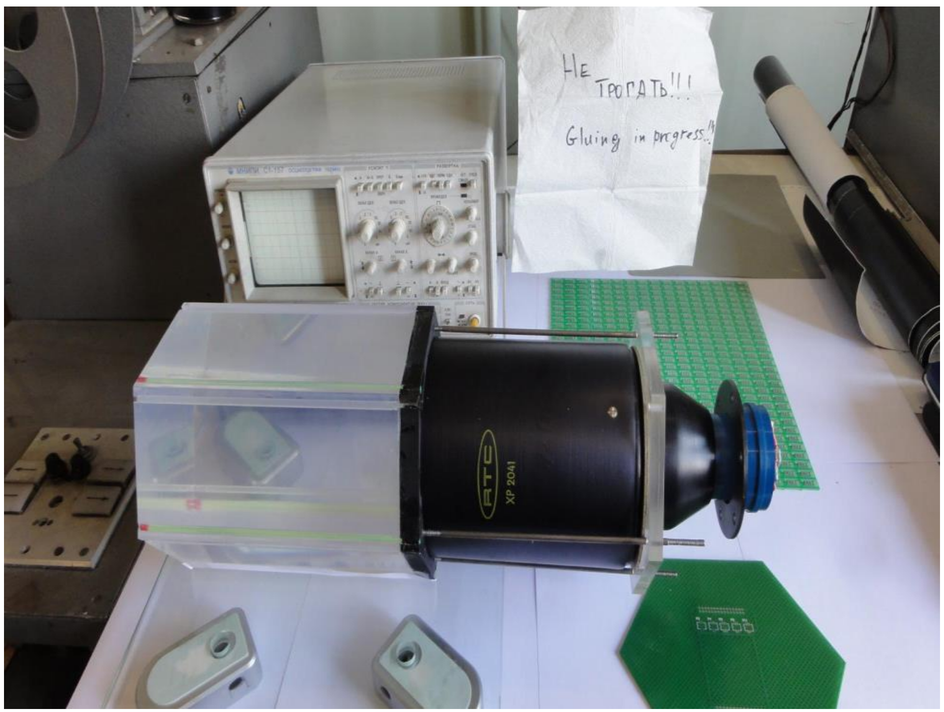

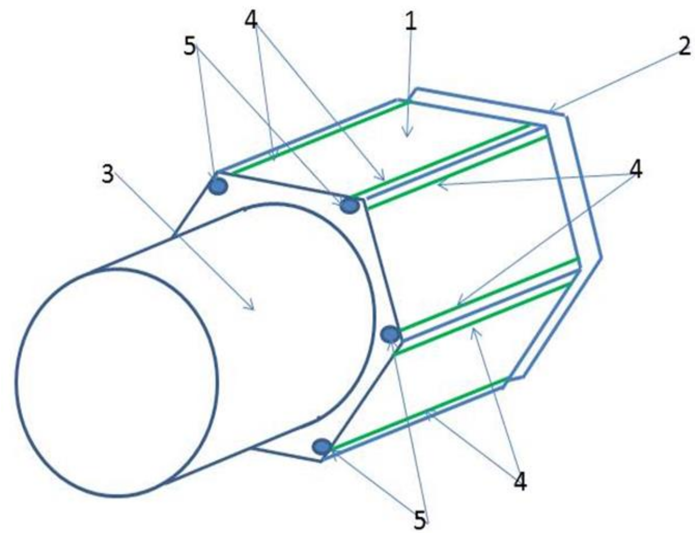

Принципиальная схема модуля. 1-блок сцинтиллятора, 2-вето детектор,3-фотоумножитель PMT RTC XP 2041, 4-пучки светосмещающих волокон, 5-SiPM

Dependence of maximum deviation protons from deposit energies (neutron energy 150 MeV)

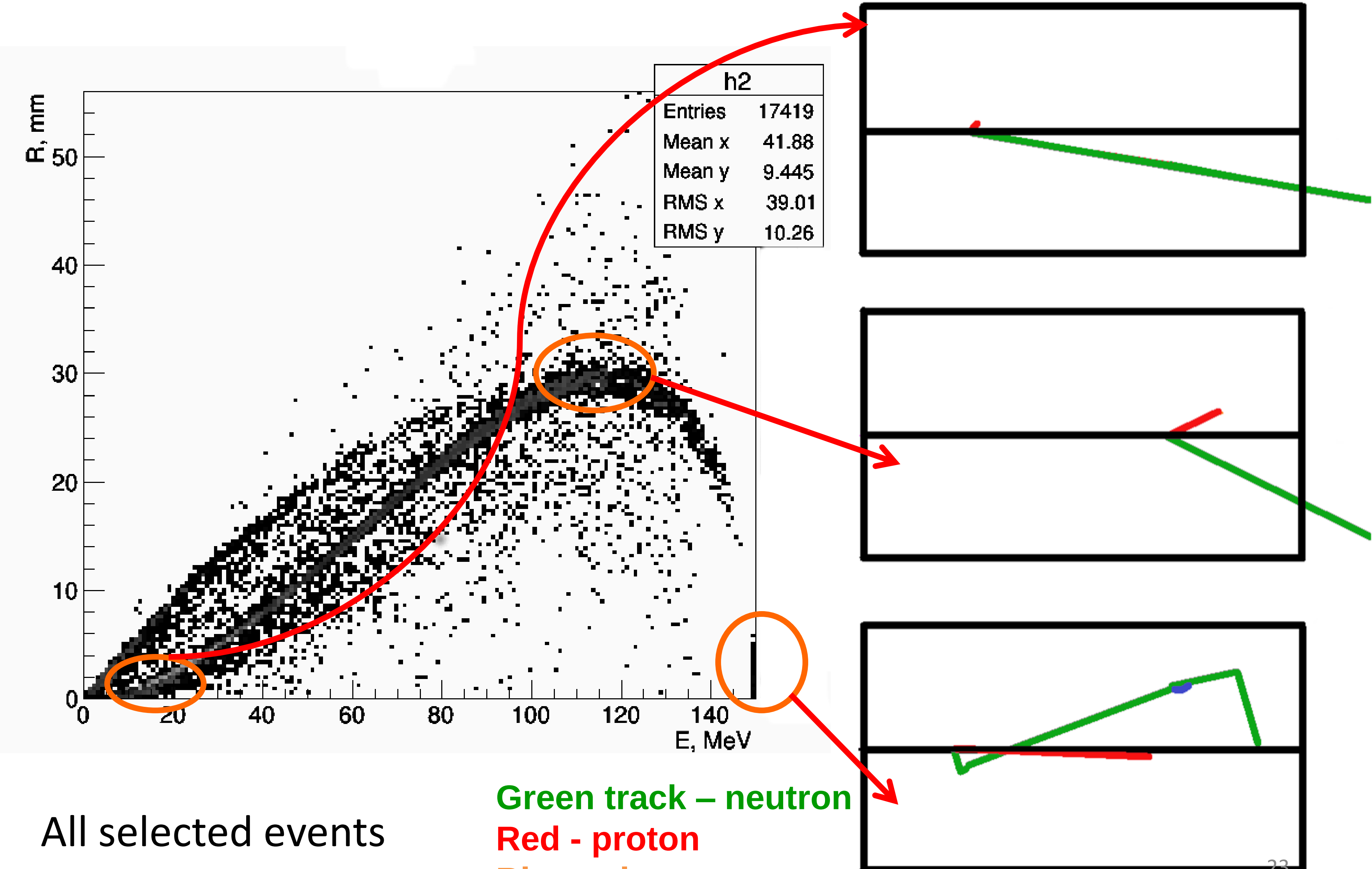

All selected events

Green track – neutron
Red - proton
Blue - electron

Схема расположения диодов детектора

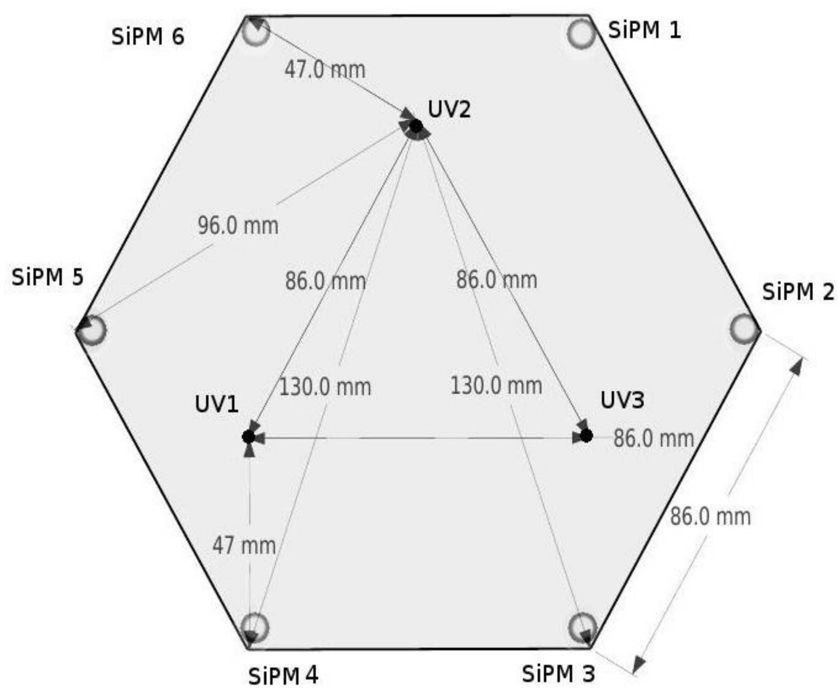

LED-collimator: A(LED)~MIP
PMT* divider~SiPM
A=A0-PED,
LED calibration:
k(LEDj)=П(i=1,…6)Ai(LEDj)
SiPM calibration
K(SiPMi)=П(j=1,2,3)A(SiPMi)

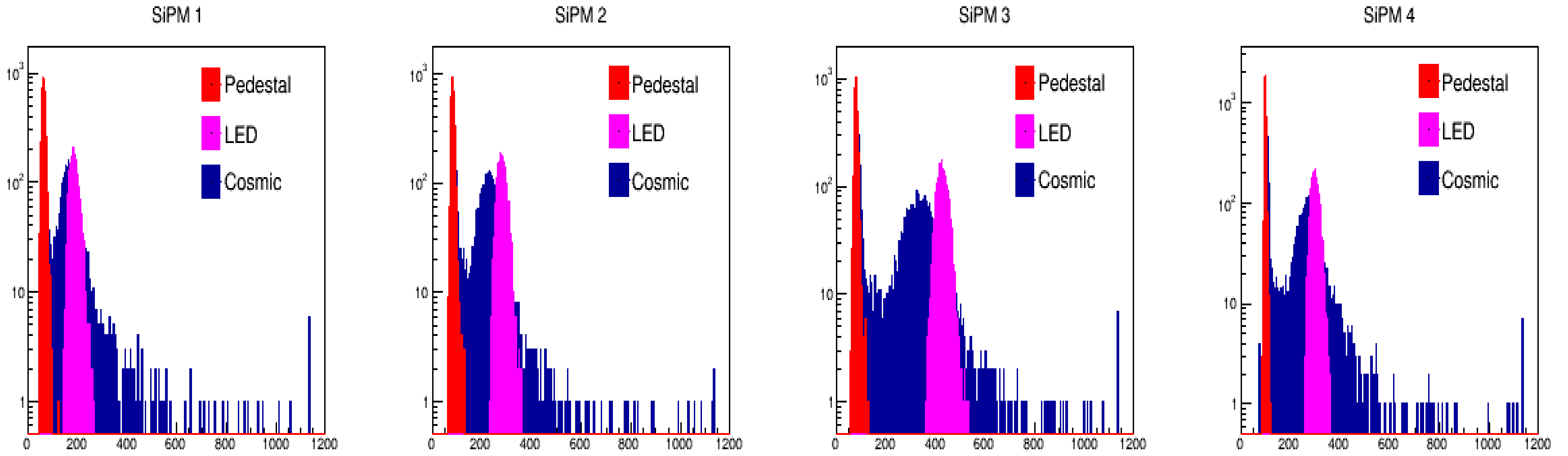

LED : 2
cosmic:central
position

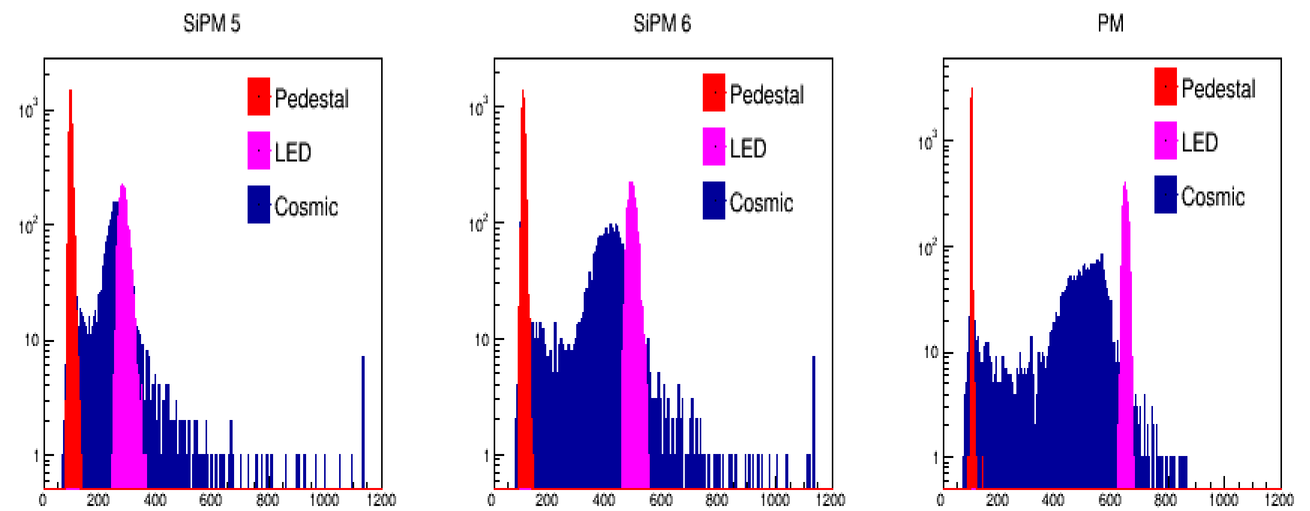

СХЕМА РАСПОЛОЖЕНИЯ ДЕТЕКТОРОВ НА КОСМИЧЕСКОМ СТЕНДЕ

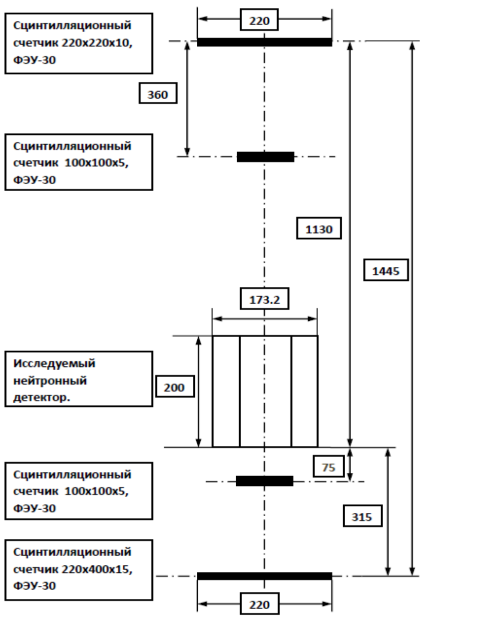

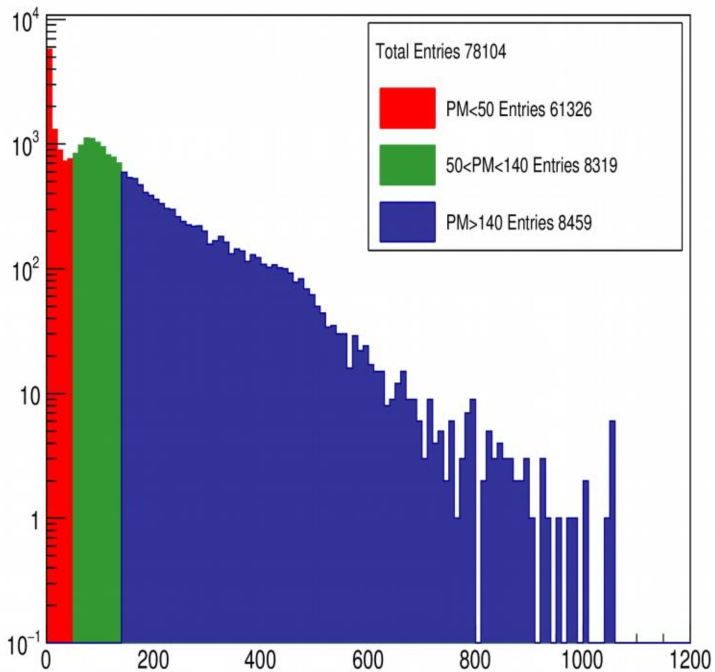

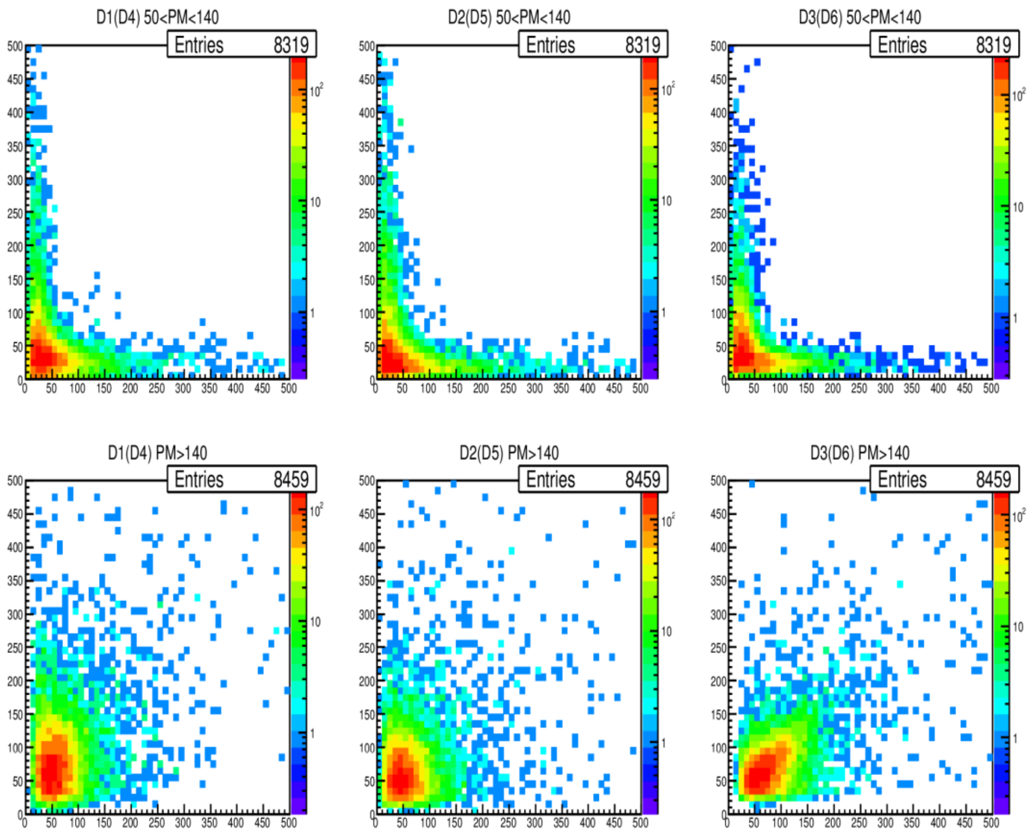

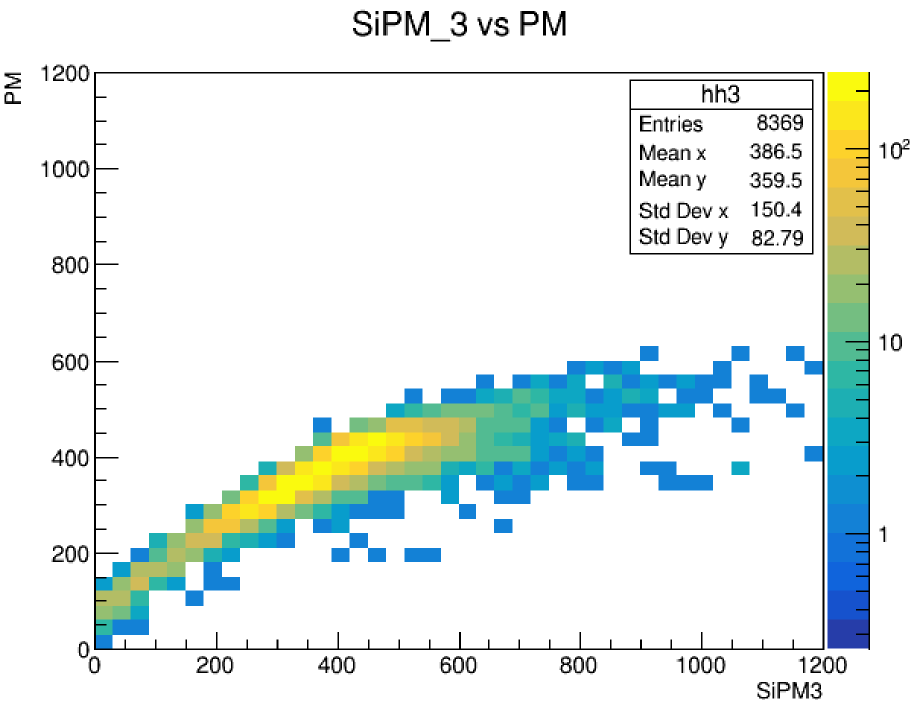
SiPM_3 vs PM
hh3
Entries 8369
Mean x 386.5
Mean y 359.5
Std Dev x 150.4
Std Dev y 82.79
PM
SiPM3

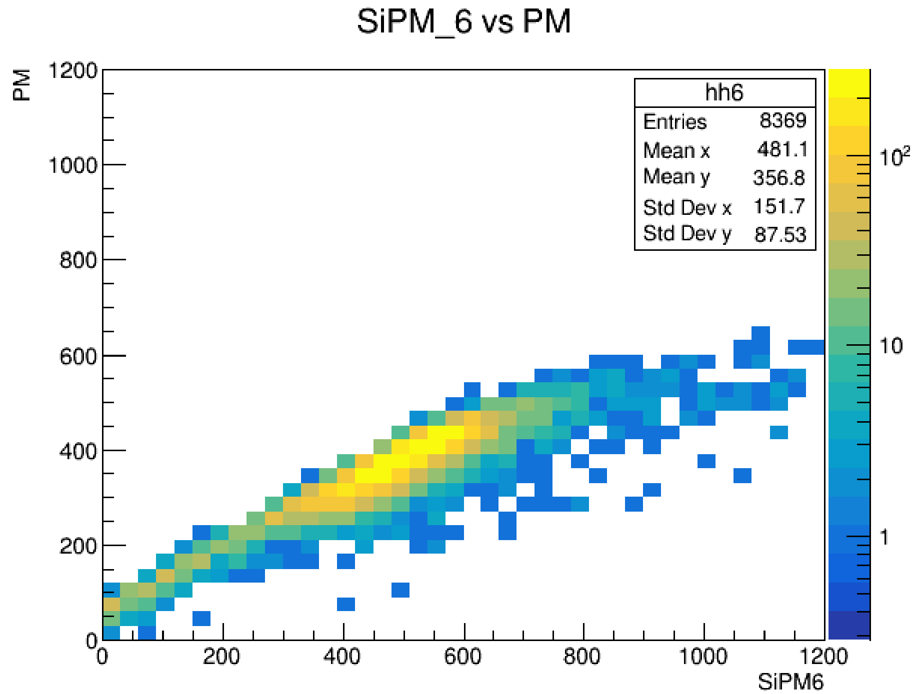
SiPM_6 vs PM
hh6
Entries 8369
Mean x 481.1
Mean y 356.8
Std Dev x 151.7
Std Dev y 87.53
PM
SiPM6

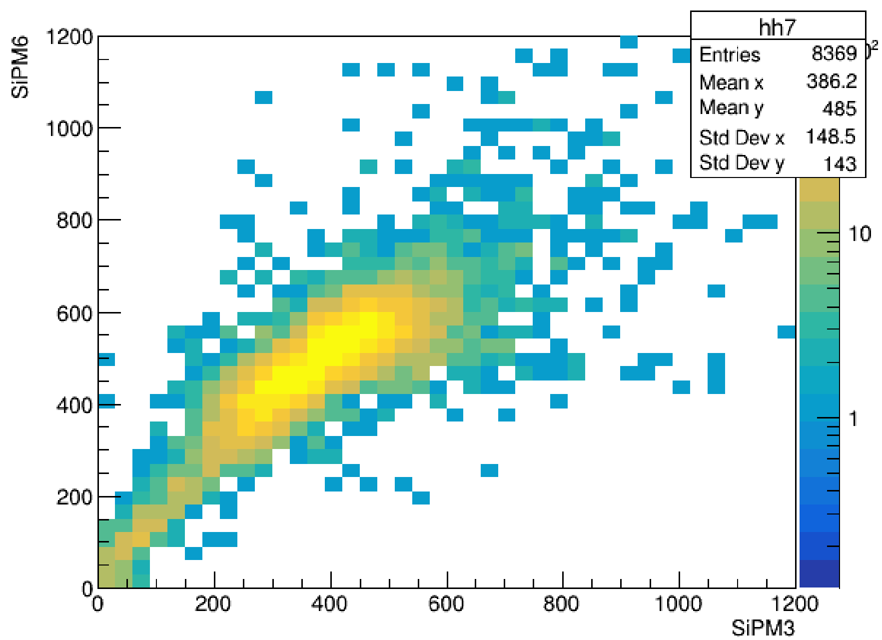
hh7
Entries 8369
Mean x 386.2
Mean y 485
Std Dev x 148.5
Std Dev y 143
SiPM6
SiPM3

Spin Physics Detector (SPD)

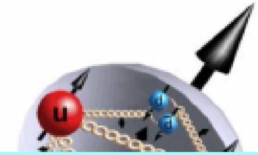

Physics tasks

Timeline

- open a project for the **SPD design:** Jan. 2019
- preparation of **CDR:** 2019
- preparation of **TDR** (+ prototyping); stage I: 2020 – 2022
  stage II: 2023
- construction of the detector: 2022 – 2025
- first measurements: 2025

- *spin effects in production of hadrons with high p_T*

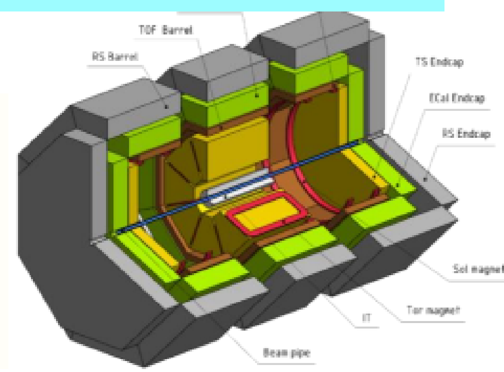

Polarized beams

- **p↑p↑** at $\sqrt{s_{pp}}$ **= 12 - 27 GeV, L_{av}** ≈ 10^{32} cm^{-2}s^{-1}
- **d↑d↑** at $\sqrt{s_{NN}}$ **= 4 - 13 GeV**
- *longitudinal and transverse polarization in SPD and MPD*

SPD/NICA will provide a unique opportunity ***not available at other facilities***
to study all **the eight nucleon PDF** in one experiment
and obtain comprehensive information on the nucleon spin structure
at high statistical level and with minimal systematic uncertainties.

NICA Collision place for SPIN physics (deuteron and other beams, the first time all isotope states for NN system: pp, pn,nn.)

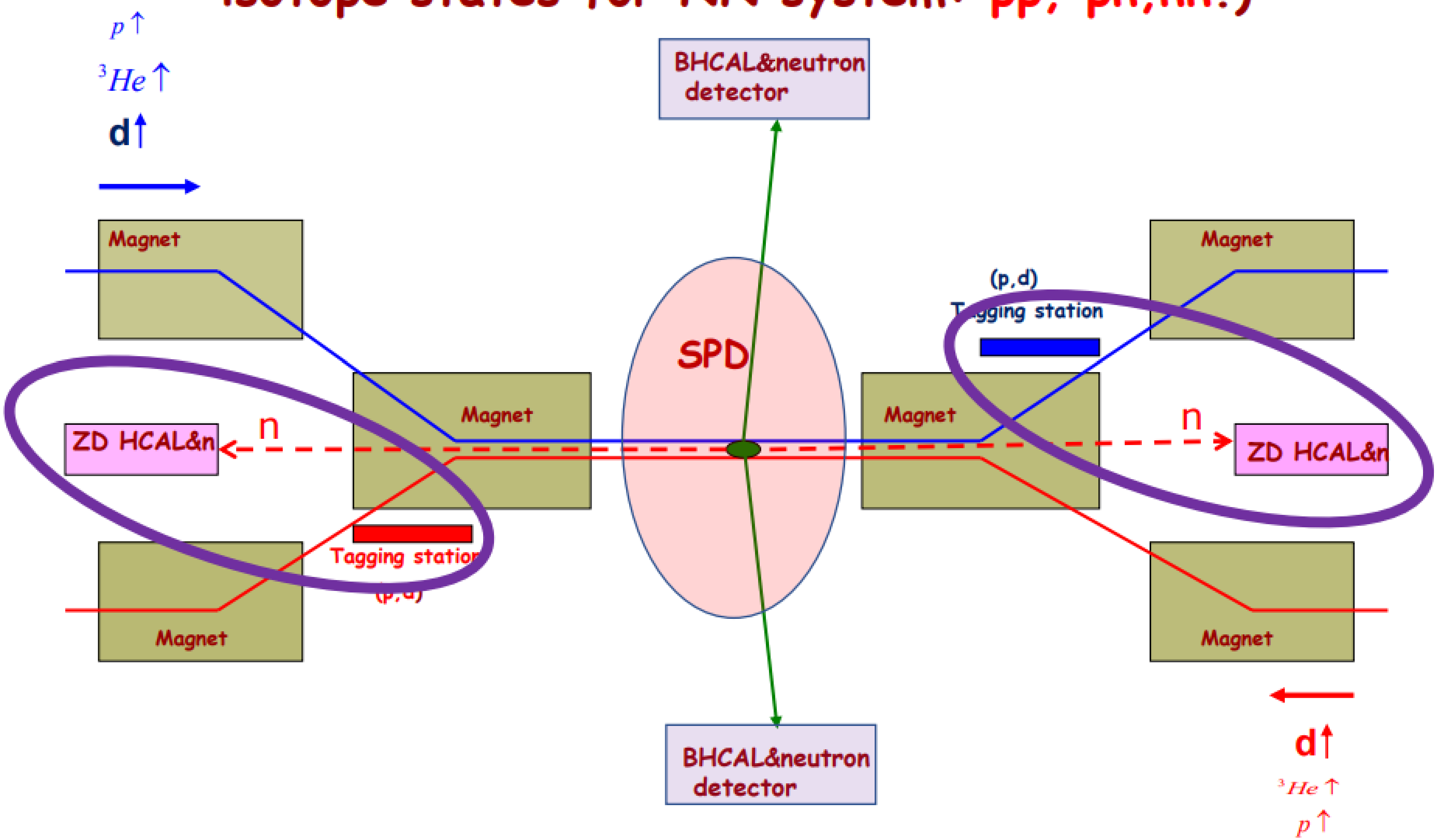

The tagging stations can be used as polarimeter!

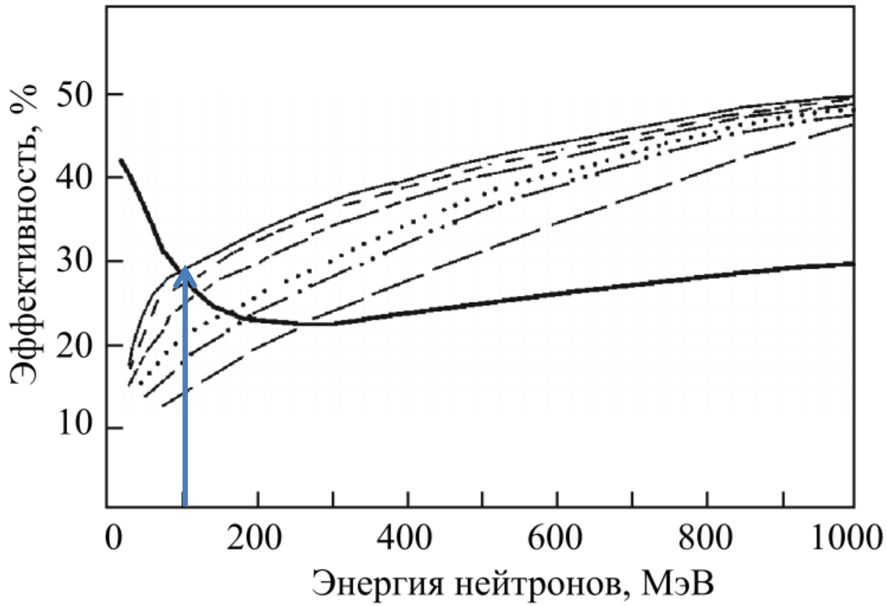

Рис. 19. Вычисленные эффективности для структуры железо–сцинтиллятор толщиной 20 см как функция кинетической энергии нейтронов для различных толщин слоев $d =$ 0,5, 1, 2, 5, 10 и 25 мм (толщина железа равна толщине сцинтиллятора, эффективность понижается с увеличением d). Толстой сплошной кривой показан расчет для чистого сцинтиллятора [114]

114: Blaich Th. et al. Nucl.Inst.Meth.A, 1992, v.314,p.136

Стартовая конфигурация (7.2.2018, A.S.)

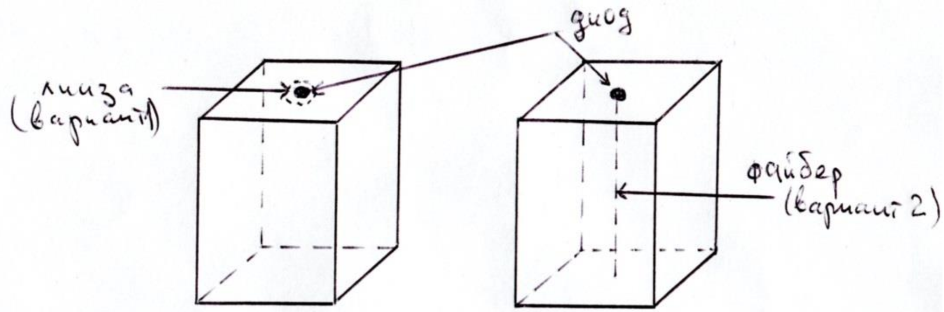

64×30 = 1920 диодов
15см Pb + 90 см сцинтиллятора (~1,5+1,1 яд. дл.)
(~30 + 2 рад. дл.)

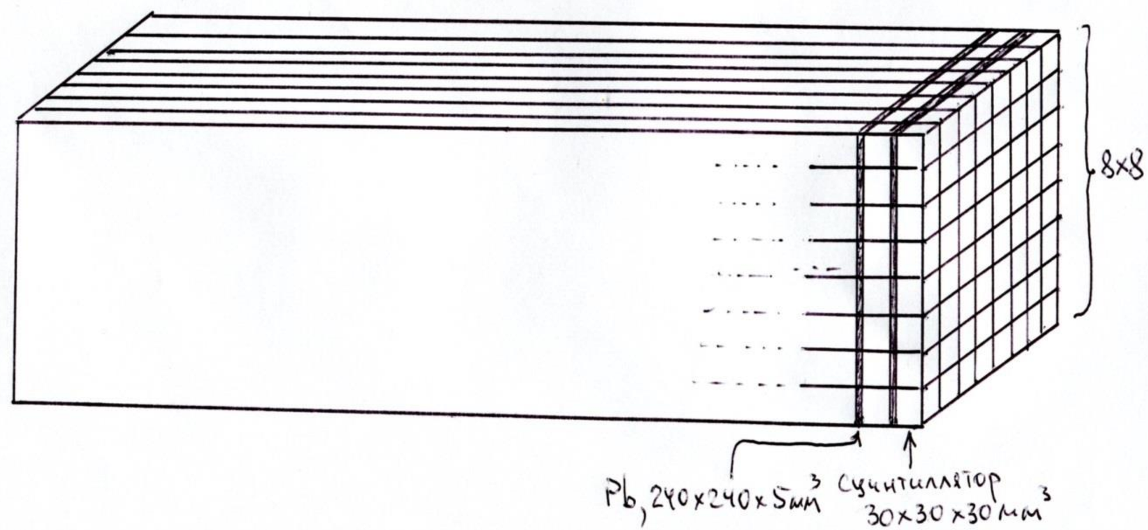

габариты 1050×240×240 мм³
30 слоев

Калориметр SPD

Калориметр состоит из 30 слоев, состоящих из ячеек 8x8 по 30x30x30 мм сцинтиллятора и слоев свинца 240x240x5 мм между ними

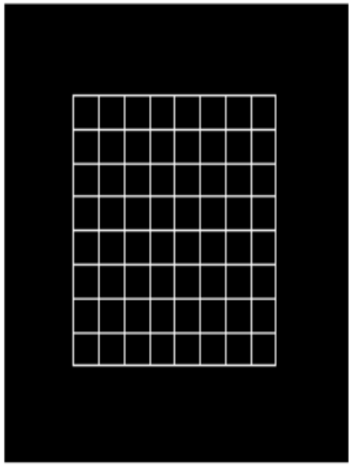

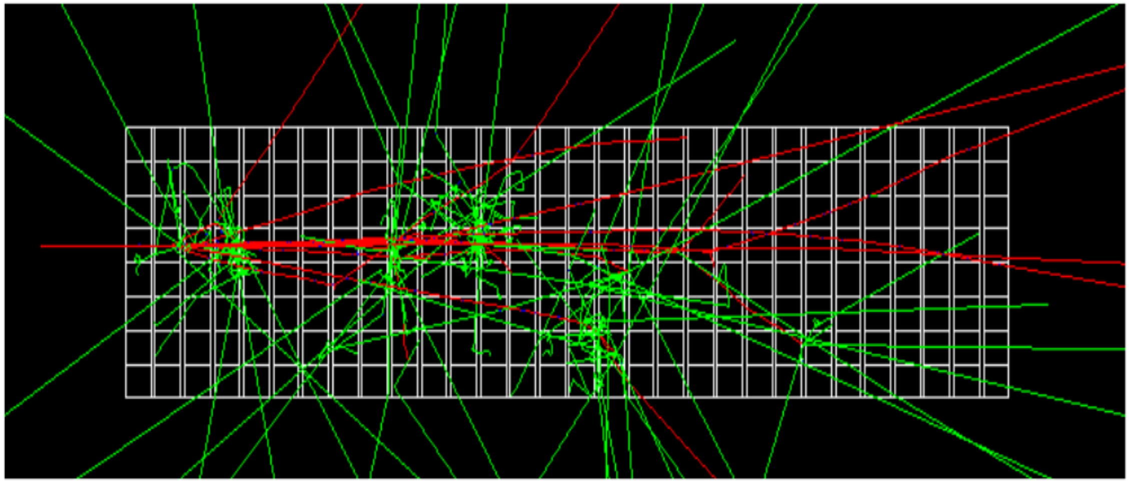

Д.Кирин (ИТЭФ), М.Парайпан(ОИЯИ)

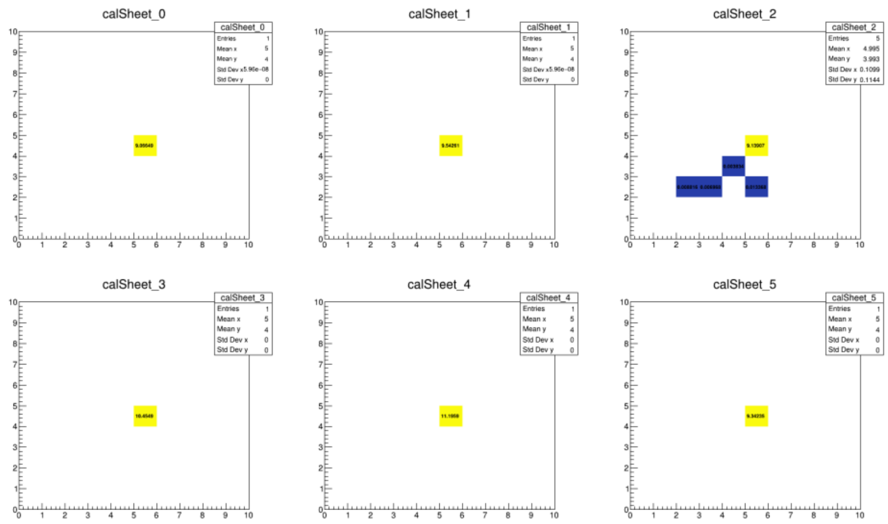

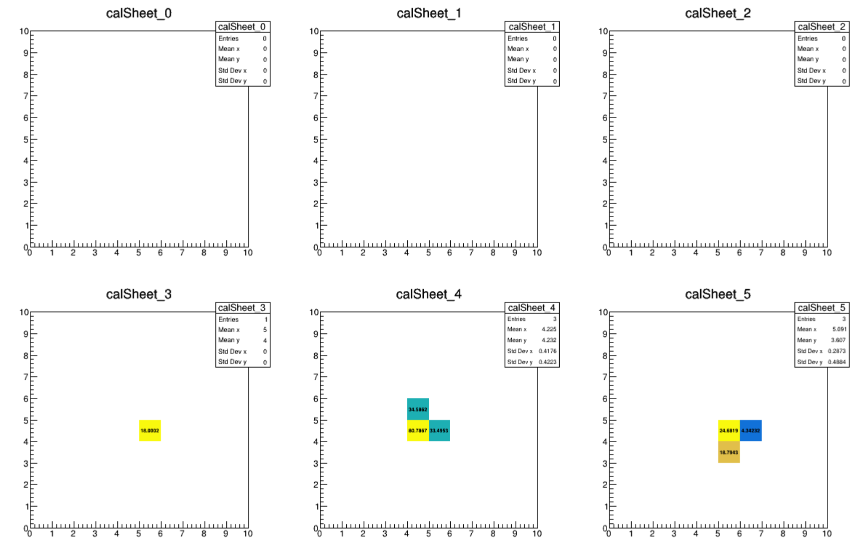

Proton ↔ Neutron (T=1GeV)

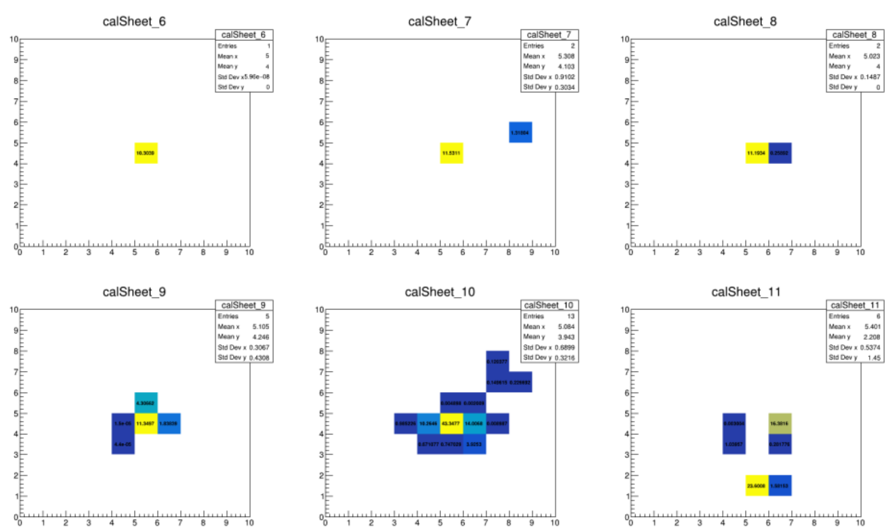

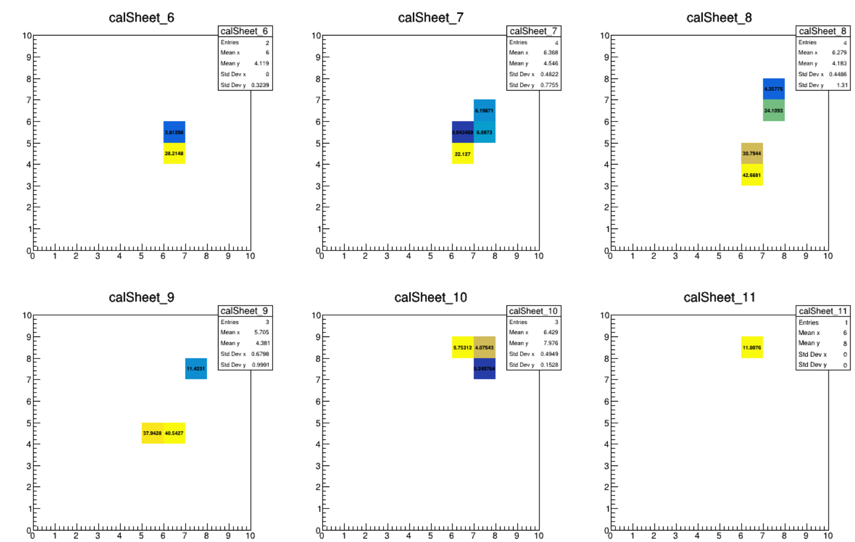

Proton ↔ Neutron (T=1GeV)

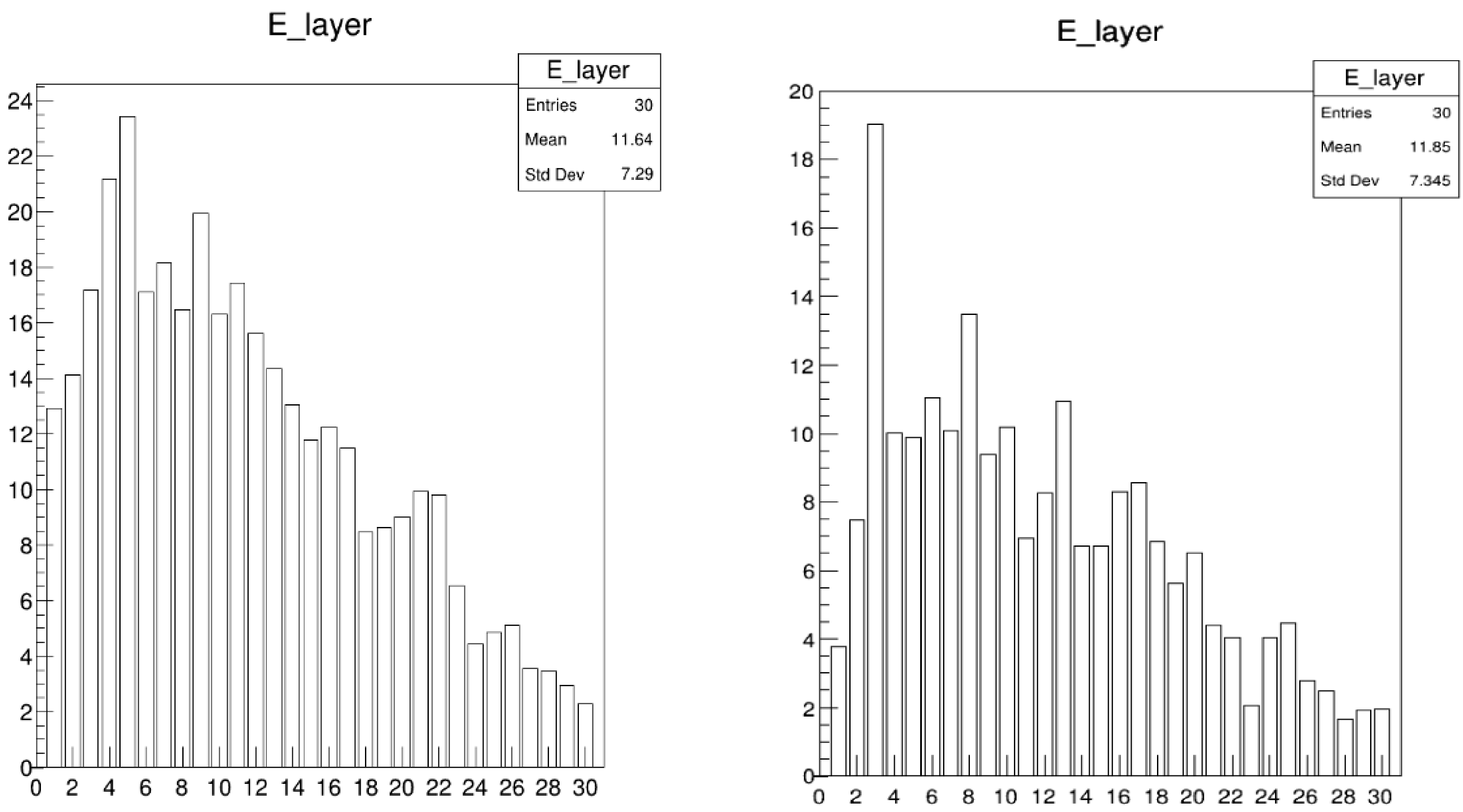

The final NeuLAND design is based on a fully active detector of organic scintillator material. However, in the past also an alternative scheme using passive converters and a multi gap resistive plate chamber (MRPC) based detector had been investigated in detail, including the construction and test of a fully operational 2 m long prototype. The scintillator-based design shows significantly better performance than the MRPC option, therefore it is adopted for the technical design of NeuLAND.

For the MRPC-based neutron-detector prototype, a setup similar to LAND is used, but the scintillator is replaced with an MRPC. As converter material, stainless steel is selected for practical reasons. In an MRPC, a charged particle passing through a gas volume causes ionization. Owing to the electrical field strength of $\approx$100 mV/cm, an avalanche is caused by this ionization. The mirror charge of the avalanche on a readout electrode is used as signal. MRPC's are well-known for their excellent time resolution, as low as σt= 20 ps for special configurations [An-08].

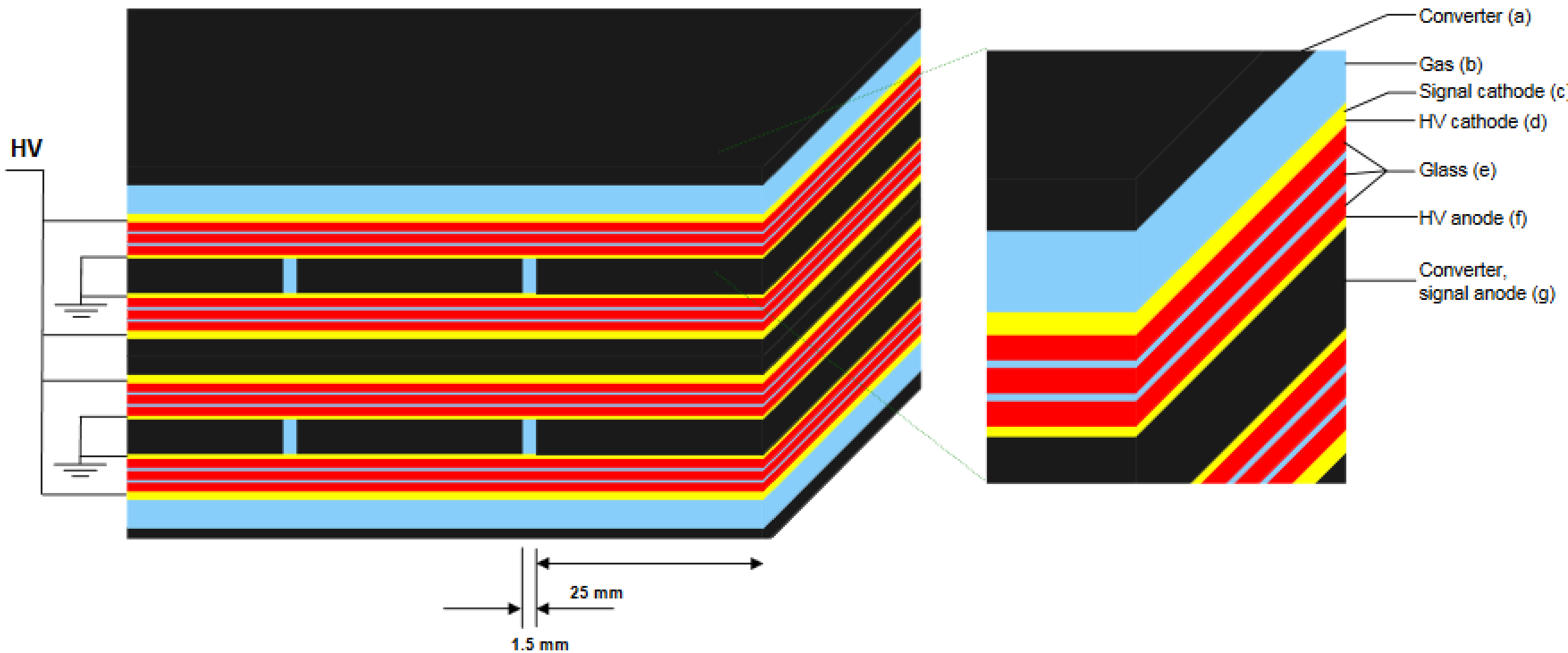

Figure B.1.: Schematic cutout of a neutron detector MRPC module, as seen from one of the sides where the signals are read out. From top to bottom, a 2 mm thick stainless steel converter plate (a), a gas volume (b). Subsequently, the signal cathode formed by copper strips applied on mylar foil (c), and the high voltage cathode given by mylar foils with one-sided antistatic coating(d). The 1 mm thick float glass sheets (e) form a symmetrical 2×2 gap structure. The high voltage anode (f) is from the same material as the high voltage cathode. The central 4 mm thick signal anode strips (g) also serve as converter for the subsequent lower half of the MRPC structure. The gas volumes (b) between signal cathode and outer converter serve to reduce cross-talk between cathode strips. Incident neutrons are converted to charged particles

Выводы:

1) Холодный и плотный угол фазовой диаграмы-новая перспективная область исследований
2) Значительную и содержательную часть вторичных частиц в этой области составляют нейтроны или частицы, распадающиеся на нейтроны
3) В детекторах нейтронов качественно новый этап начинается в связи с развитием технологий SiPM и MRPC
4) На этом этапе будут востребованы специалисты широкого спектра, включая разработчиков алгоритмов идентификации нейтронов

Обзор по нейтронным детекторам:

Юревич В.И., ЭЧАЯ, 2012,т.43, вып.3,стр.709

Распределение энергии по слоям и модулям для нейтронов 1 ГэВ

Толщина слоя свинца 5 мм

По слоям

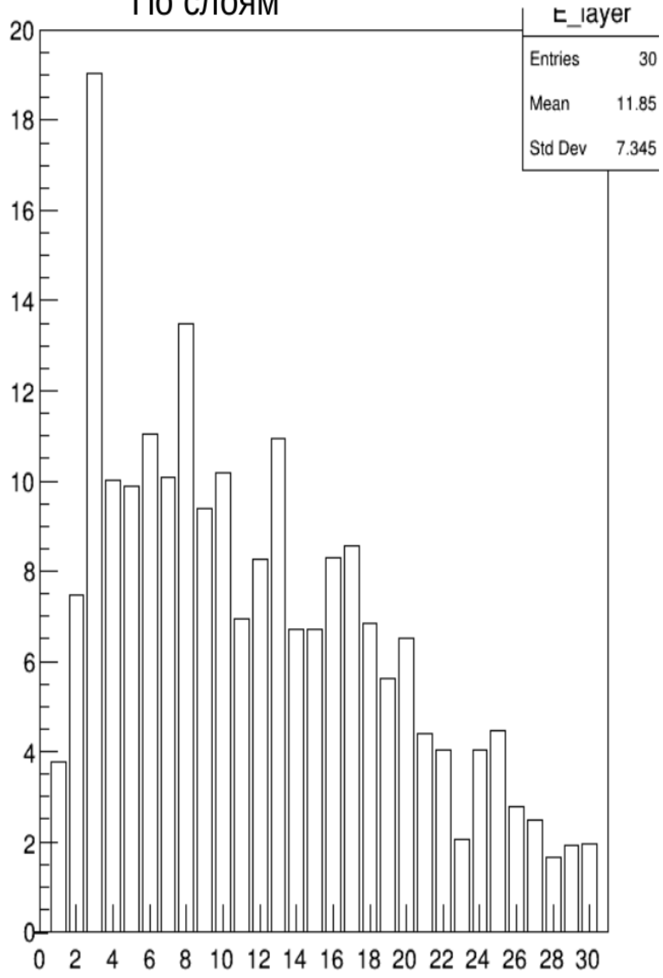

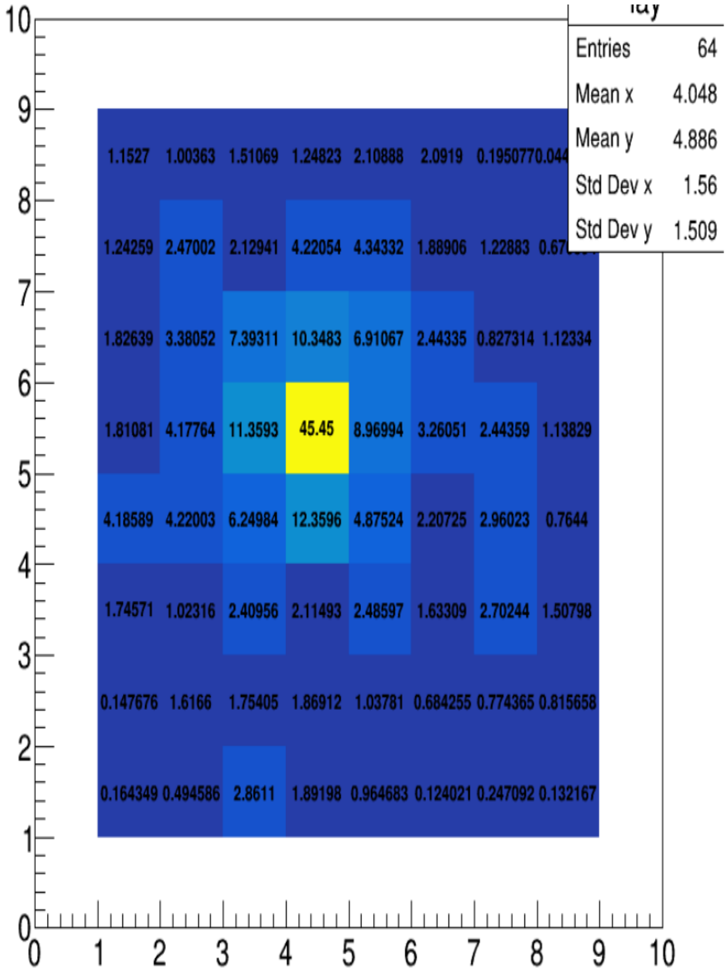

Phase diagram of nuclear matter

*current region of the experiments

**$\rho/\rho_0 \gg 1$,

$T/T_0 \ll 1$(DenseColdMatter):

rich structure of the QCD phase diagram - new phenomena are expected!

***Diagram study not finished- additional new

phenomena can be found

See, for example L.McLerran, “Happy Island”, arXiv:1105.4103 [hep-ph] and ref. therein.

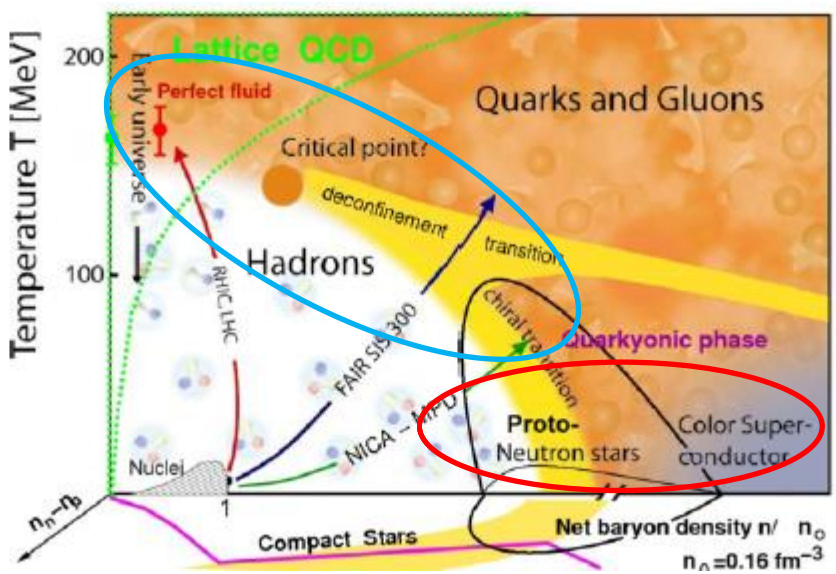

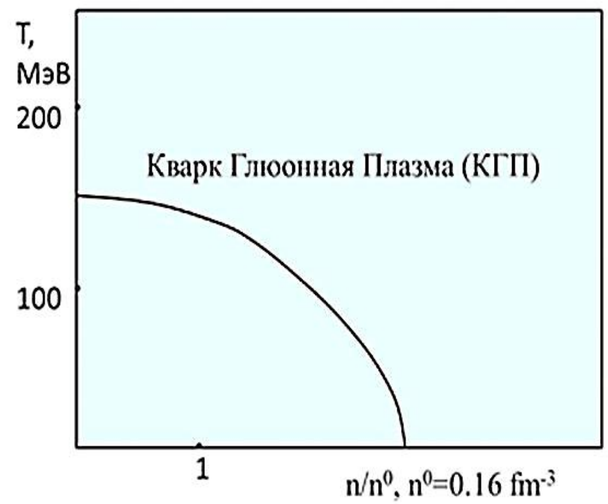

Рис.1. Представление о фазовой диаграмме ядерной материи 80-х годов прошлого века.

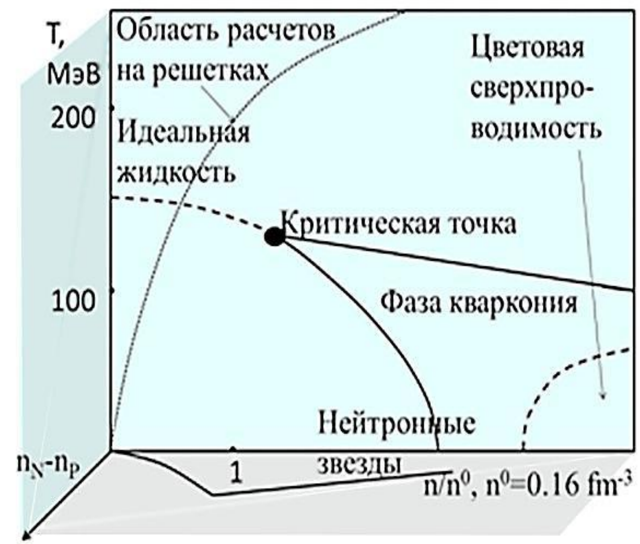

Рис.2. Современный вид фазовой диаграммы.

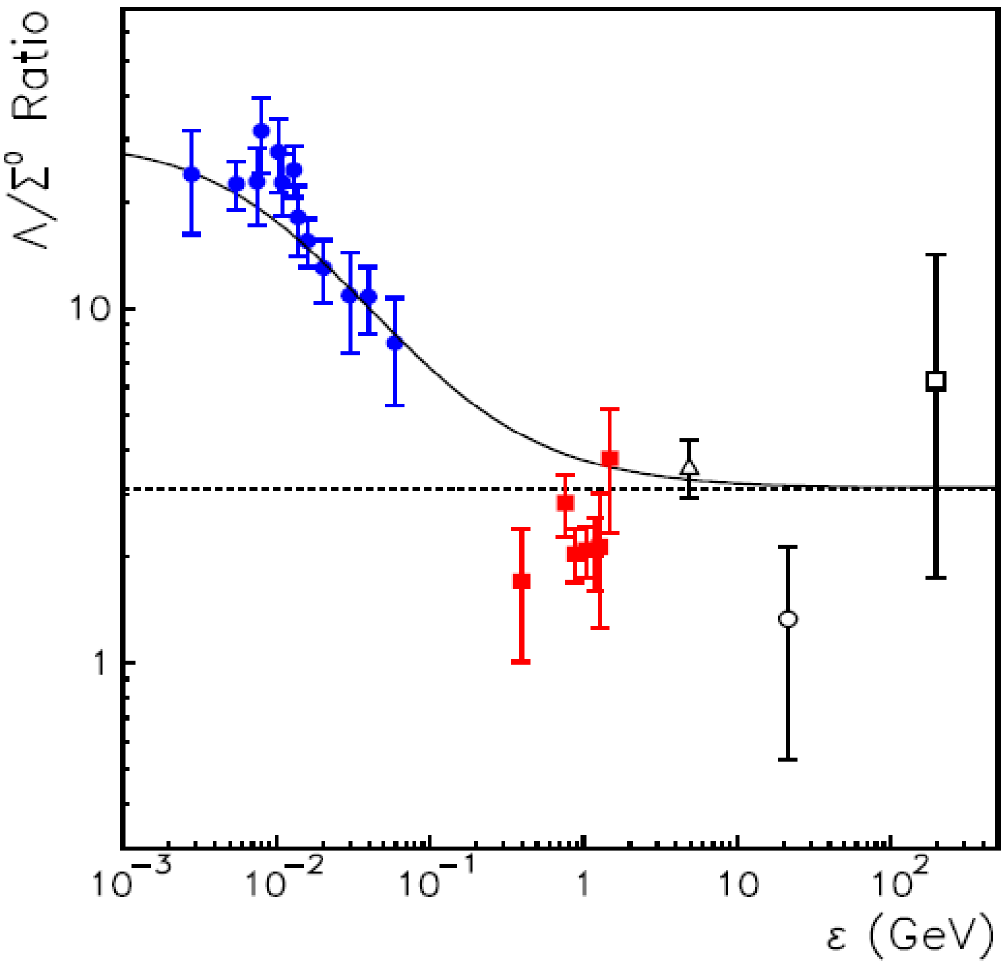

Fig. 3. The Λ/Σ^0 cross section ratio as a function of the excess energy ϵ. The solid circles show the ratio obtained for the $pp \to K^+\Lambda p$ and $pp \to K^+\Sigma^0 p$ reactions at COSY [2]. Solid squares are pp results from Ref. [25]. The open triangle and open circle are ratios measured in $p\,$Be [28] and $p\,$Ne [29] collisions, respectively. The open square is the result from a $d\,$Au experiment [30]. The curves are cross section ratios based on the $pp \to K^+\Lambda p$ results with Λp FSI (solid line) and without FSI (dashed line).

"It is interesting to observe that the ratios for nuclear targets, measured at high energies, are roughly in line with the results from high-energy pp collisions. Unfortunately, the new and still preliminary STAR result is afflicted by large uncertainties and, thus, precludes any firm conclusion concerning a possibly larger ratio with respect to that found in the pp interactions. Several authors have pointed out that the experimental ratio of around 3 coincides with the ratio of the isospin multiplicity of the Λ and Σ's [2,28,30]. But we are not aware of any deeper reason why those two quantities should be connected."

arXiv:hep-ph/0608098, A.Sibirtsev et al.

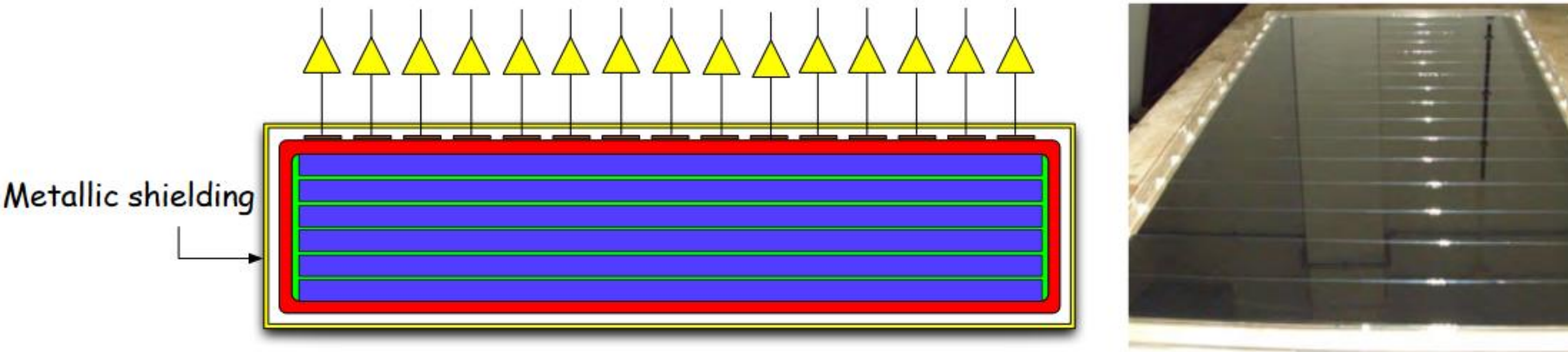

Figure B.11.: Schematic drawing (left) and photograph (right) of the iron-less RPC module with the readout electrodes.

B.7. MRPC Solution using Glass as Converter As an alternative, a new concept for the detection of high energy neutrons based on RPC's was also proposed. This concept considers only glass as converter material. There is no iron in the whole detector. Based on a modular geometry, each RPC module contains a certain number of glass electrodes separated by 300μm, operated in a standard gas mixture. The gas gaps are encapsulated in a gas tight plastic box, which only contains feed-throughs for the active gas (a standard mixture of 90% freon and 10% SF6) and the high voltage. The readout strips are allocated outside the plastic box. The whole system is electrically isolated by a metallic shielding. Based on simulation studies using the R3BROOT framework, the thickness of the glass plates has been chosen to be 3 mm [Mac-11]. A schematic view of the iron-less RPC concept is shown in the left panel of figure B.11. A RPC module(100 cm×50 cm) based on the iron-less RPC concept already exists at LIP-Coimbra, and it can be seen in the right panel of figure B.11.

Femtoscopy.

Λ: $\Sigma(1385) \rightarrow$ $\Sigma^0 \rightarrow \Lambda\gamma(100\%)$, $\Lambda\pi(87\%)$, $\Sigma\pi(12\%)$, $\Xi^0 \rightarrow \Lambda\pi^0(99.5\%)$, $\Xi^- \rightarrow \Lambda\pi^-(99.9\%)$

P: $\Lambda \rightarrow p\pi^-(64\%)$, $\Sigma^+ \rightarrow p\pi^0$ (52%), $\Sigma^0 \rightarrow \Lambda\gamma(100\%) \rightarrow p\pi^-(64\%)$

$a_{pp}(^1S_0)$=-7.8 fm; $a_{np}(^1S_0)$=-23.7 fm; $a_{nn}(^1S_0)$=-16.4 fm.

$a_{p\Lambda}(^1S_0)$=-2.7 fm; $a_{\Sigma+p}(^1S_0)$=-3.85 fm; $a_{\Lambda\Lambda}(^1S_0)$=-0.88 fm[1]

[1] Th.A.Rijken, M.M.Nagels, Y.Yamamoto,
Progress of Theoretical Physics Suppl.N0.**185**(2010),14

To mesure Λp, better to know $\Sigma^0 p$, $\Sigma^+\Lambda$, ΛΛ, $\Sigma^0\Lambda$ interactions.

SiPM 1

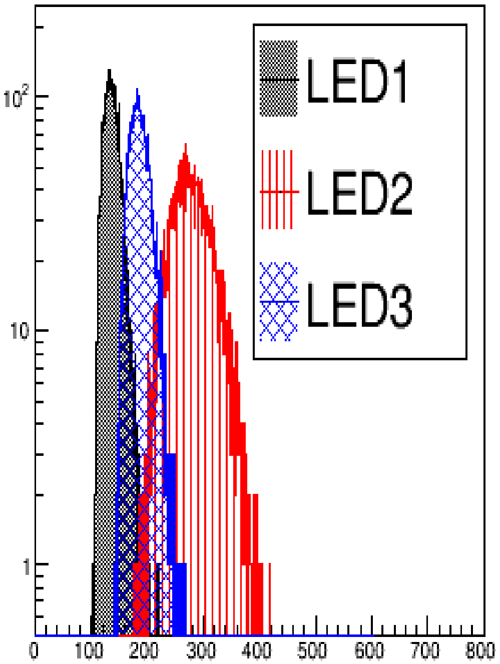

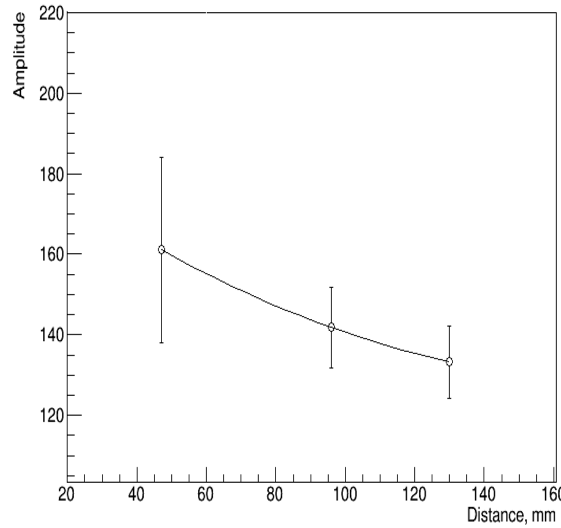

SiPM 3

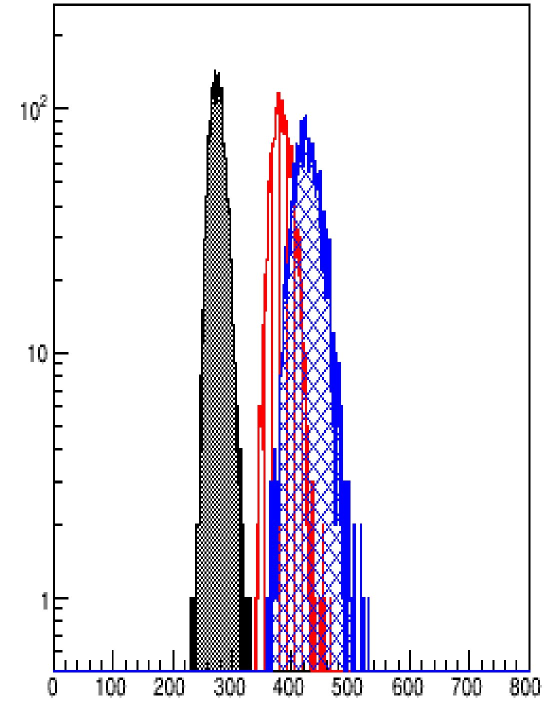

PM

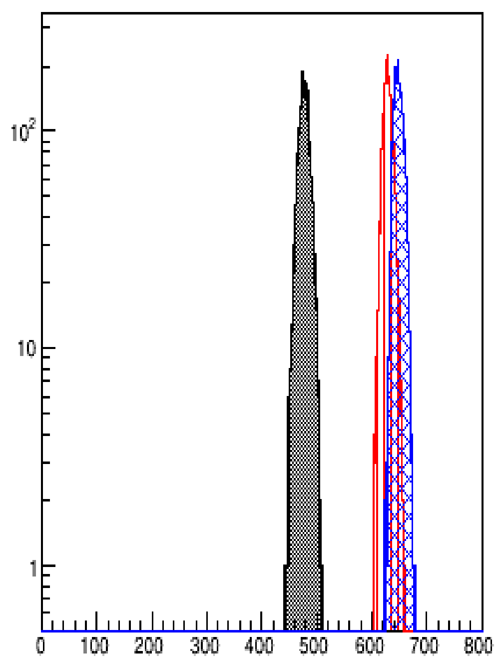

LED-collimator: A(LED)~MIP

PMT* divider~SiPM

A=A0-PED,

LED calibration:

k(LEDj)=Π(i=1,…6)Ai(LEDj)

SiPM calibration

K(SiPMi)=Π(j=1,2,3)A(SiPMi)

How the new state of matter is created in the lab?

Y. Ivanov, V. Russkikh, V.Toneev,
Phys. Rev. C73 (2006) 044904

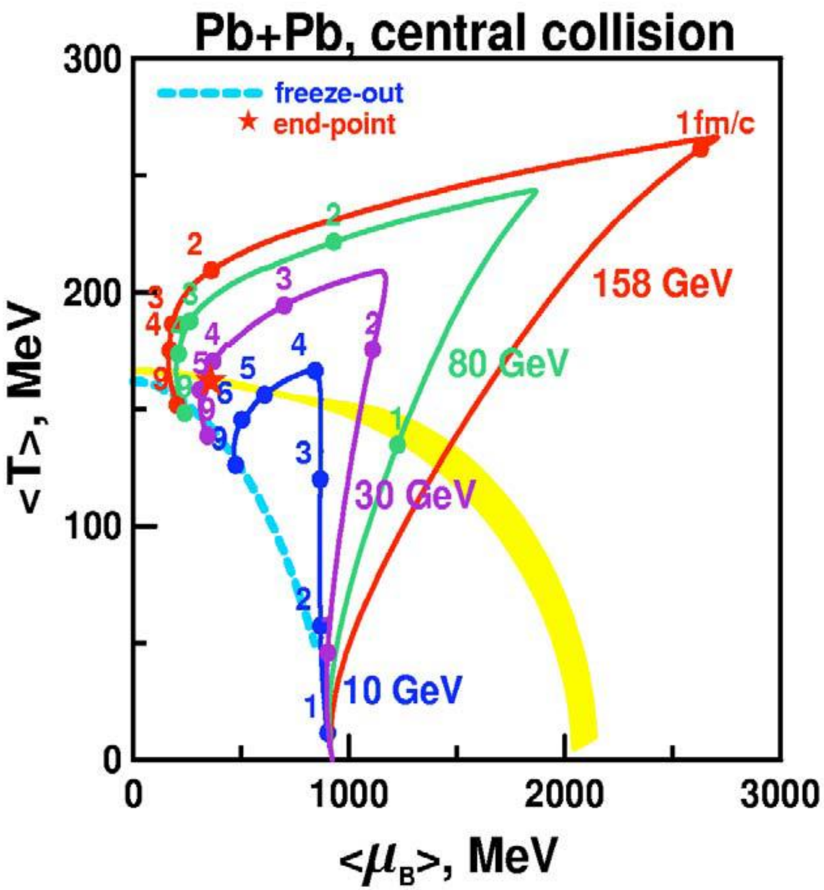

The QGP can be created by heating matter up to a temperature of 2×10^{12} K, which amounts to 175 MeV per particle. This can be accomplished by colliding two large nuclei at high energy (note that 175 MeV is not the energy of the colliding beam). Lead and gold nuclei have been used for such collisions at CERN and BNL, respectively. The nuclei are accelerated to ultrarelativistic speeds and slammed into each other. When they do collide, the resulting hot volume called a "fireball" is created after a head-on collision. Once created, this fireball is expected to expand under its own pressure, and cool while expanding. By carefully studying this flow, experimentalists put the theory to test.

*Region $\rho/\rho_0 \gg 1$, $T/T_0 \ll 1$(DenseColdMatter) hardly accessible experimentally by standard way

Phase diagram*

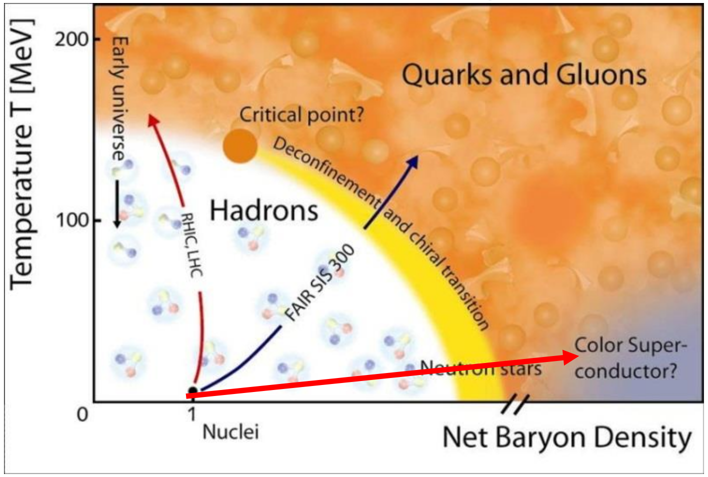

*http://www.gsi.de/forschung/fair_experiments/CBM/

Scheme of process

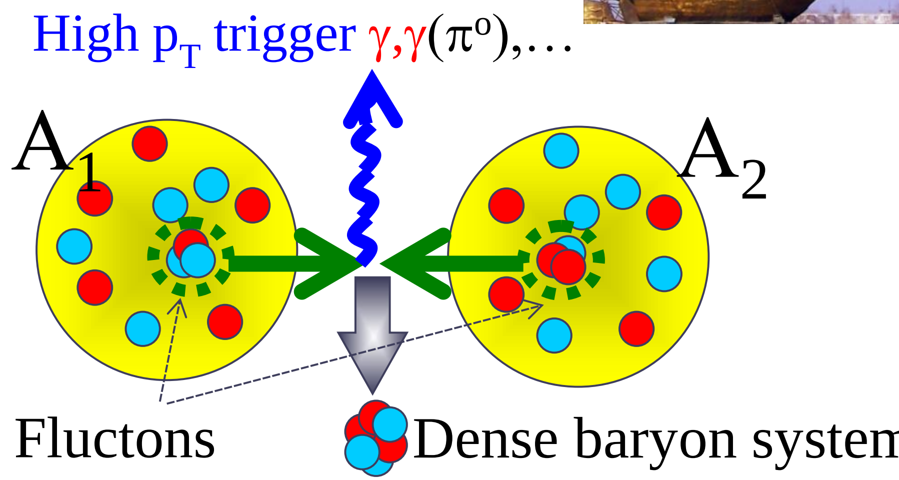

Kinematical limits for different subprocesses:
1N+1N(black line)
1N+Flucton(2N,3N,4N)&Flucton+1N(blue lines)
Flucton+Flucton(red lines)

He+He @ 6 AGeV

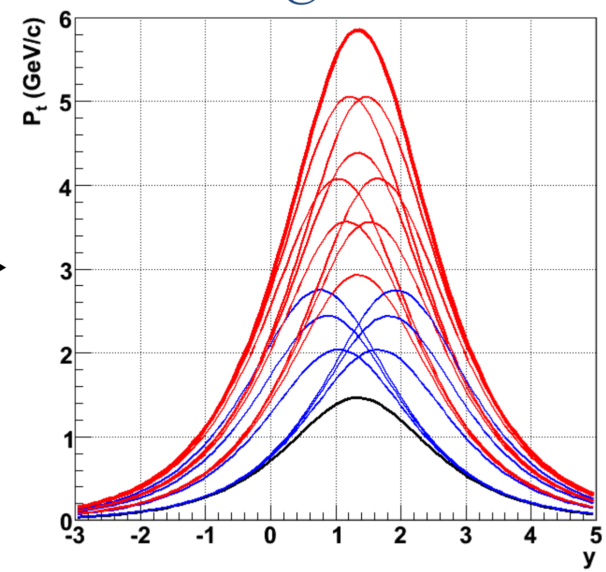

I.G.Alekseev et al.,Phys.At.Nucl.71,1848(2008), Phys.At.Nucl.78,936(2015)